A GRATING-TUNABLE EXTERNAL-CAVITY LASER BASED ON A SEMICONDUCTOR LASER DIODE

A thesis for the degree of
MASTER OF SCIENCE

Presented to
DUBLIN CITY UNIVERSITY

By
BRIAN KEVIN HURLEY B.Sc
School of Physical Sciences
DUBLIN CITY UNIVERSITY

Research Supervisor: Dr. Martin O. Henry
External Examiner : Dr. Frank Mulligan

June 1993

Acknowledgements

I would like to thank my research supervisor Dr Martin Henry for his guidance and encouragement during the course of this project Thanks are also due to Ger Sherlock at BTRL Ipswich for supplying the laser diodes used and Optronics Ireland for funding this work

I must also acknowledge the help and support of my family throughout my time in college Thanks also to the postgrads and others who helped keep it all together Thanks!

Declaration

I hereby certify that this material, which I now submit for assessment on the programme of study leading to the award of Master of Science is entirely my own work and has not been taken from the work of others save and to the extent that such work has been cited and acknowledged within the text of my work

Signed 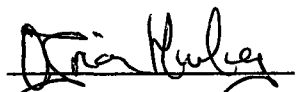

Brian K Hurley

Date 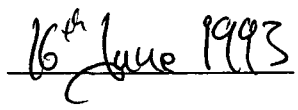

Contents

Table of Figures

Abstract.

Conventional semiconductor laser diodes have found limited applications in the areas of spectroscopy and sensors due to their multimode output and relatively large linewidth Although single mode operation is possible with the use of distributed feedback techniques this tends to be at the expense of tunability However operation of a laser diode in an external cavity gives a tunable narrow-linewidth source ideal for spectroscopic and sensing applications

This work details the design and construction of a tunable external-cavity semiconductor diode laser The external reflector used is a diffraction grating operating in the Littrow geometry The collimated first order diffracted beam is focused on the antireflection coated facet of a British Telecom Research Laboratory 1 3μm laser chip 55cm away

The cavity has been characterised using a 1m focal length grating monochromator and a Fourier transform infrared spectrometer The laser behaved in the predicted manner exhibiting a greatly reduced lasing threshold current and single mode operation The device showed a grating tunable range of 37nm with intermode tuning, achieved by current change, of 10 GHz / mA A device linewidth of 3 3kHz was calculated and was found to be in good agreement with both calculated and measured results for similar configurations

Chapter 1: Introduction

1.0 Introduction.

The purpose of this chapter is to provide a general introduction to the topic of semiconductor laser diodes In particular the characteristics of laser diodes when operating in an external cavity are discussed The general types and features of different cavity schemes are presented along with their various applications The chapter commences with a brief description of lasing action in general and progresses to the specific case of lasing action in semiconductor materials

1.1 Lasing action.

The word laser is an acronym for *L*ight *A*mplification by the *S*timulated *E*mission of *R*adiation Consider the atomic levels E_1 and E_2 in Figure 1 1 below Radiation of suitable energy $E = h\nu = E_2 - E_1$, where h is Planck's constant and ν is the frequency of the radiation, can interact with the atomic system in one of three ways

a) Absorption A photon may be absorbed by an atom in the lower energy state E_1 causing it to be excited into the higher energy state E_2

b) Spontaneous emission An atom in level E_2 can de-excite from E_2 to E_1 with the emission of a photon with energy $E = h\nu = E_2 - E_1$

c) Stimulated emission A photon of energy hν, incident on an atom in the excited state E_2, may cause the atom to decay to the lower energy level E_1 with the emission of a photon This emitted photon will have the same phase and direction as the incident photon

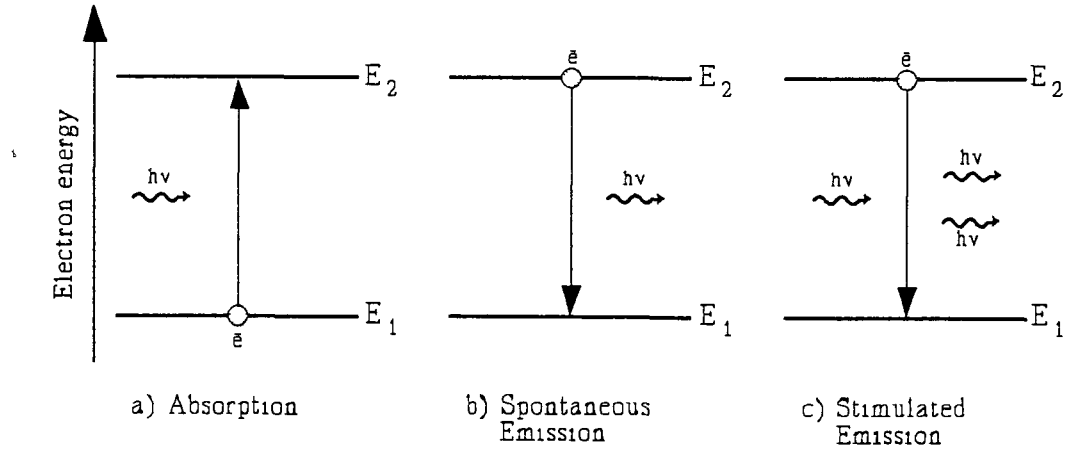

Figure 1 1· The three types of optical transitions.

It is obvious that a net gain in photon flux can only occur if the probability of stimulated emission is greater than the probability of absorption. This situation can only happen if the population of the state E_2 is greater than that of E_1, ie. a population inversion must exist between the two lasing levels.

If the gain medium is placed between two reflectors ie. a Fabry Perot cavity, as in Figure 1.2, and the population inversion is maintained by some external pump (optical, electrical) then it is possible to reflect the stimulated radiation many times in a closed system with continuous gain over the path. If one of the reflectors is made partially reflecting and the round trip losses (losses due to absorption, scattering, off-axis propagation and the output beam itself) equal the round trip gain a useful beam may be produced. In addition, the disturbance propagating within this cavity takes on a standing wave configuration determined by the separation of the mirrors. This standing wave must satisfy the condition that the cavity length must be an integer number of half wavelengths. Since there can be several wavelengths which satisfy this condition for a given cavity length this leads to the formation of longitudinal modes, a feature predominant in semiconductor laser diodes.

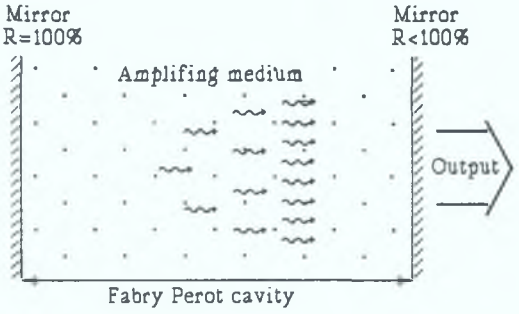

Figure 1.2: Fabry-Perot based optical amplifier.

1.2 Stimulated emission processes in semiconductor materials.

The main difference between electrons in semiconductors and electrons in other laser media is that in semiconductors all the electrons occupy, and thus share, the whole crystal volume while in conventional lasers (e.g. Ruby) the electrons are localised to their parent ion and these do not communicate with those other ions.

In a semiconductor, because of the spatial overlap of their wavefunctions, no two electrons can be placed in the same quantum state, i.e. possess the same eigenenergy (neglecting spin). Each electron must possess a unique spatial wavefunction and associated eigenenergy. This satisfies the Pauli exclusion principle. These electron

energies cluster in bands separated by forbidden energy gaps In an insulator the energy gap between the highest filled level (the valence band) and the lowest empty level (the conduction band) is great enough that the electrons cannot be transferred across by thermal excitation, thus current cannot flow However in a semiconductor the gap is small and, at room temperature, electrons can be thermally excited from the valence band (VB) to the conduction band (CB) The crystal can therefore conduct electricity The degree of conductivity can be controlled not only by temperature but also by doping Doping is the process whereby impurity atoms are added to the semiconductor crystal during manufacture to provide either an excess of electrons (n-type) or an excess of holes (p-type) This introduces new energy levels into the device and changes its electrical characteristics The radiative transitions which can take place within these bands in a semiconductor play a very similar role to the electronic transitions mentioned previously in Section 1 1 In both cases electrons participate in the same three types of optical interaction, namely, absorption, spontaneous and stimulated emission In a direct band gap semiconductor, (indirect bandgap semiconductor materials are not used in laser diode fabrication due to the predominance of non-radiative decay mechanisms), in thermal equilibrium the CB usually contains only a few filled states and the VB only a few vacant states The electrons in the CB have a probability of falling into the VB, in the process of which a photon is created by spontaneous emission When a photon of suitable energy passes through such a semiconductor it has a high probability of being absorbed and passing its energy to one of the many electrons in the VB However it can also stimulate an electron in the CB to decay to the VB with the emission of a stimulated photon This photon has the same phase and is emitted in the same direction as the incident photon In thermal equilibrium this event has a very low probability of occurrence due to the small number of electrons in the CB However with excitation by other means e g a drive current, the number of electrons in the CB can be made to exceed the number of holes in the VB This is the process of 'pumping' the laser into an inverted state Therefore the probability of photon generation by stimulated emission can be made greater than that of absorption This condition is the one of population inversion mentioned in Section 1 1 and it is this that provides optical gain It should also be noted that the considerable number of electrons in the CB retain their capability of random recombination and so the inverted state of the semiconductor is characterised

also by a high rate of spontaneous emission

The change from a limited number of individual pairs of localised electronic states, as in Section 1 1, to the large number of relatively unlocalised states in the bands of a semiconductor results in a change in the lasing properties of the system [1]

- The higher concentration of electronic states in the bands of a semiconductor provides the capability of higher gain
- Greater interaction between the excited states in the same band leads to a rapid refilling of the empty states caused by de-excitation This almost instantaneous redistribution of carriers leads to very high rates of energy generation
- In a semiconductor the electronic states may be transported through the material by diffusion or conduction This makes it possible to invert the material by the direct injection of carriers at a p-n junction
- For semiconductors, due to the large number of energy levels present the possibility exists for a considerable number of transitions

A semiconductor that is pumped into an inverted state provides gain to a propagating wave but it will not cause laser oscillation until it is enclosed within an optical resonator This resonator reflects a proportion of the photons back into the inverted region For lasing to start the stimulated emission from the inverted medium must compensate for the loss of photons at the output and elsewhere Therefore laser oscillation occurs abruptly where the pump level is increased to the point (known as the threshold) where the photon balance is first fulfilled This threshold current is an important device parameter and its minimisation is often sought A typical light versus current, (LI), curve is shown in Figure 1 3 The threshold point can clearly be seen After threshold there is a linear increase in light intensity The reflection from the ends of the optical resonator provide maximum feedback at a specific set of wavelengths which satisfy the Fabry-Perot condition of the cavity The

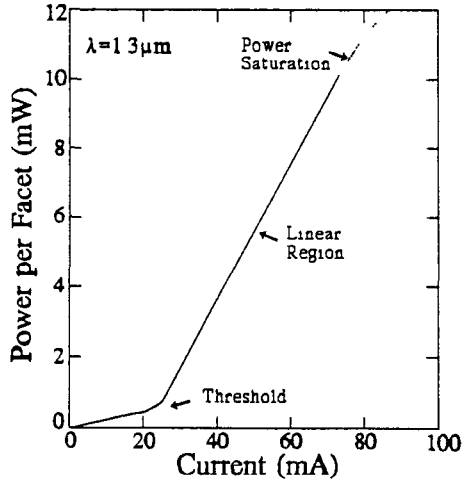

Figure 1.3: Typical efficiency curve for InGaAsP laser diode.

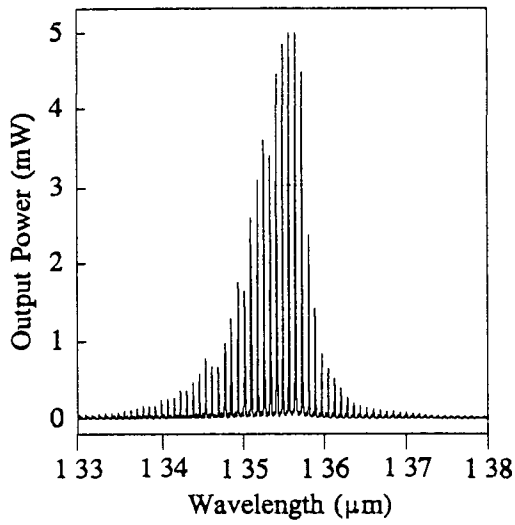

Figure 1.4: Laser spectrum showing mode structure.

optical field distributions at these wavelengths are called longitudinal modes In a laser diode, optical feedback is provided by the cleaved facets of the semiconductor material which act as mirrors, reflecting the light back and forth inside the gain medium Since the optical gain is high, relatively low facet reflectivities will suffice The typical value for the refractive index of a semiconductor used in laser diode production is 3 5 This leads to a residual reflectivity of approximately 35%, which is sufficient to sustain lasing action A typical longitudinal mode spectrum is shown in Figure 1 4

1.3 Development of semiconductor laser diodes.

Semiconductor lasers operating in the wavelength range 1 1-1 65μm can be fabricated using indium gallium arsenide phosphide (InGaAsP) on an indium phosphide (InP) substrate Room temperature operation of InGaAsP-InP lasers was first reported in 1976 [2] A schematic diagram of this broad area laser is shown in Figure 1 5 This, however, was not the first report of lasing action in semiconductor materials

The first laser diode was demonstrated in 1962 [3] just three years after the first laser was produced These first semiconductor lasers were homogeneous gallium arsenide (GaAs) p-n junctions The chip had a metallic base with a wire contact on the top The two output facets were polished to provide feedback while the side facets were roughened to prevent laser oscillation in that plane These devices had a very high threshold current and could only be operated at cryogenic temperatures The reason for this was

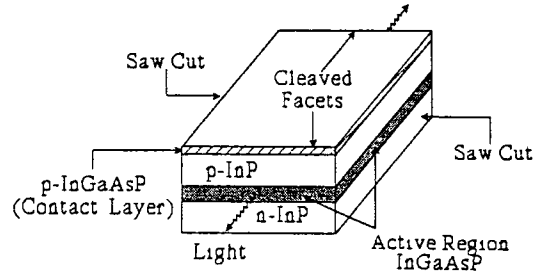

Figure 1.5: Broad area diode laser.

the lack of carrier or photon confinement These problems were overcome with the development of the heterostructure laser, i e a laser made from different semiconductor materials such as GaAs and GaAlAs The most common type of heterostructure laser is the double heterostructure These are made from materials that have different band gap energies for current confinement and different refractive indices for photon confinement

In a double heterostructure laser the optical mode is confined perpendicularly to the junction plane For stable operation with a low threshold, additional confinement of the optical mode is required Lasers can be classified into two categories depending on how this confinement is achieved

(i) Gain Guided The width of the optical mode is determined by the width of the current pumped region which limits the region of optical gain

(ii) Index Guided The lasing mode is confined by the use of a narrow region of higher refractive index in the junction plane Index guided lasers may further be subdivided into two categories, namely weakly and strongly index guided

In weakly guided lasers the active region is continuous with the index discontinuity provided by a cladding layer Strongly guided lasers employ a buried heterostructure with the active region bounded by low index layers both along and normal to the junction plane

Despite the fabrication difficulties associated with index guided devices (compared with the relative ease of fabrication of gain guided devices), their lower threshold currents (typically 10-15mA for index guided compared to 100-150mA for gain

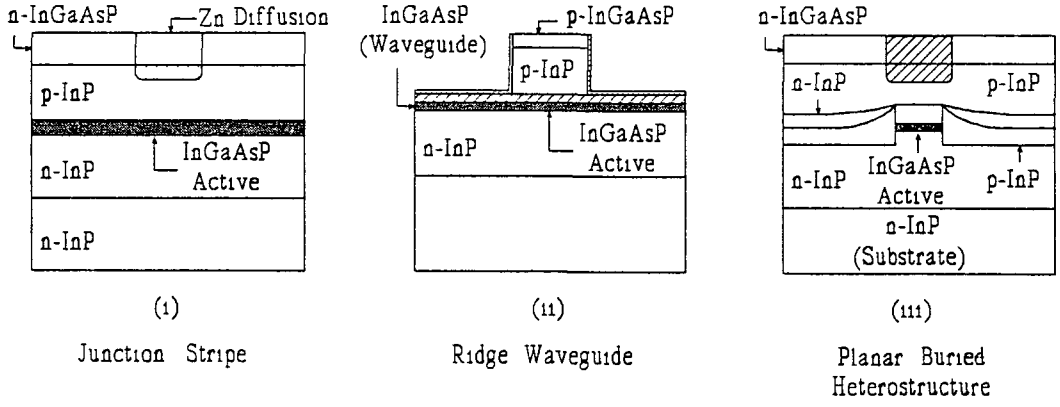

Figure 1.6: Schematic cross section of different types of laser structures: (i) gain guided: (ii) weakly index guided: (iii) strongly index guided.

guided), stable operation and good high modulation speed characteristics make them a more favoured choice especially for data transmission applications.

Depending on the specific design, these lasers are known by various names, for example, rib waveguide, ridge waveguide, channel substrate, etched mesa buried heterostructure, buried crescent buried heterostructure and strip buried heterostructure. Examples of typical laser structures are illustrated in Figure 1.6.

In the conventional Fabry Perot devices, feedback is provided by facet reflections. This reflectivity is constant for all longitudinal modes and it is this that gives rise to the multimode output associated with such devices.

Distributed feedback, (DFB), lasers [4] improve the mode selectivity by making the feedback frequency dependent. This is achieved through the use of a grating, etched so that the thickness of one of the heterostructure layers varies periodically along the cavity length. The resulting periodic perturbation of the refractive index provides feedback by means of backward Bragg scattering which couples forward and backward travelling waves. By careful choice of the grating period, such a device can be made to provide feedback only at selected wavelengths. Figure 1.7 shows a schematic diagram of a DFB laser diode.

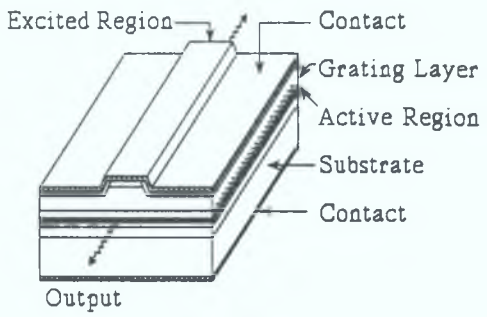

Figure 1.7: Distributed Feedback Laser (DFB) Diode.

1.4 The laser diode in an external cavity.

In the previous Section it was mentioned that DFB mechanisms can provide single wavelength semiconductor lasers with a high degree of side mode suppression. The operating wavelength is relatively insensitive to external influences since it is determined by a permanently etched grating. Although this wavelength stability is an attractive feature of such devices it is obtained at the expense of tunability. Coupled-cavity semiconductor lasers have the potential of offering mode selectivity along with wavelength tunability. Figure 1.8 shows the mechanism of mode selectivity for

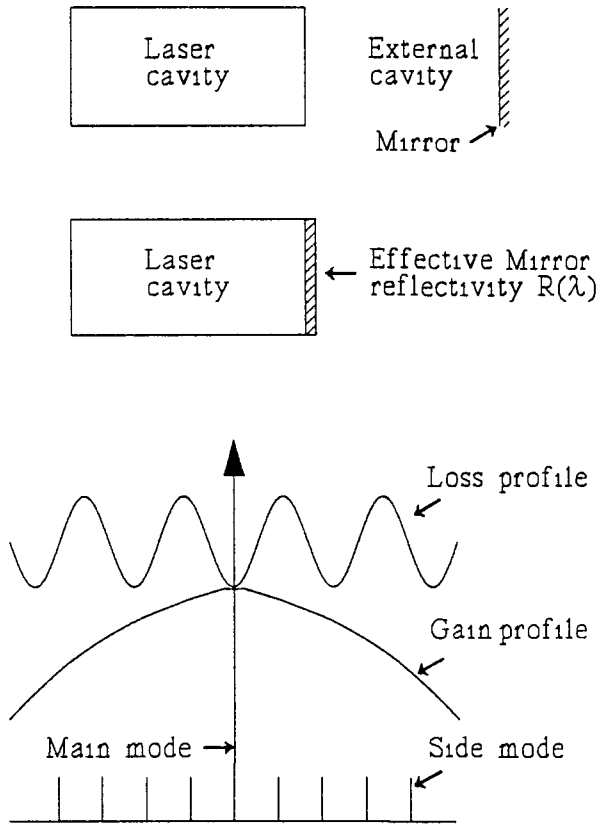

Figure 1.8: Mode selectivity in an external cavity laser system [After Ref. 1].

coupled-cavity lasers Feedback from the external cavity can be modelled through an effective wavelength dependant reflectivity of the facet facing the external cavity This results in different cavity losses for different Fabry-Perot modes of the laser cavity In general the loss profile is periodic, as shown in Figure 1 8, due to this Fabry-Perot selection The mode selected by the coupled-cavity device is the FP mode that has the lowest cavity loss and is closest to the peak of the laser medium gain profile Due to the periodic nature of the loss profile other FP modes with relatively low cavity losses may exist Such modes are discriminated against by the gain roll-off because of their large separation from each other These side modes can be further suppressed if the reflecting mirror is made highly wavelength selective by, for example, using a diffraction grating or a wavelength selective filter

An aspect of coupled-cavity lasers that has attracted much attention is their ability to exhibit a smaller CW linewidth than that of a conventionally operated device In the case of such devices the linewidth can be reduced by up to four orders of magnitude (from 100MHz to 10kHz) by placing the device in an air cavity of a few centimetres

in length [5] The reason for this linewidth reduction is the increase in photon lifetime This results in a much larger number of intracavity photons at a given output energy, therefore the single mode linewidth decreases

1.5 Coupled-cavity schemes.

Coupled-cavity semiconductor lasers can be classified into two broad categories These are active-active and active-passive depending on whether or not the second cavity can be pumped to provide gain Figures 1 9 and 1 10 show a specific example of each kind of device

1.5.1 Active-active: In the active-active scheme both sections can be independently pumped This gives an additional degree of freedom which can be used to control the behaviour of the device A natural choice is to use one active material separated by some means Cleaving and etching techniques have been used for this purpose Whichever technique is employed, the qualitative behaviour of these so called three terminal devices is similar with respect to mode selectivity and wavelength tunability The active-active scheme offers the possibility of electronically shifting the modes since both cavities can be independently controlled Usually one of the cavities, called the controller, is operated below threshold Variation in the drive current significantly alters the refractive index (RI) by changing the carrier density in the cavity This shift in RI causes a shift in longitudinal mode which results in selection of different FP modes of the cavity

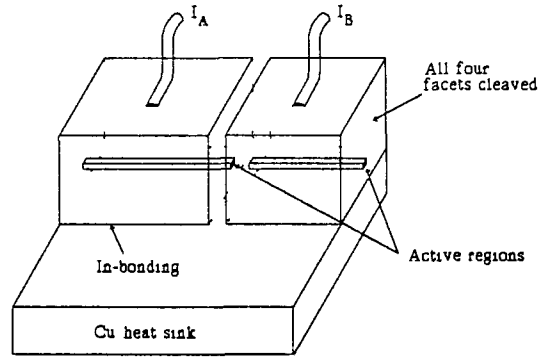

Figure 1.9: Cleaved coupled cavity laser.

1.5.2 Active-passive: In the active-passive scheme the laser is coupled to an external cavity that remains unpumped In its simplest form a mirror is placed a short distance from one of the laser facets, the facet may have an antireflection coating to increase the coupling between the two cavities In another scheme the external cavity consists of a graded index (GRIN) fibre lens, to provide greater coupling and avoid diffraction

losses In these external cavity schemes mode selectivity arises from the interference between the waves propagating in the two cavities An additional mode selective mechanism can be introduced if the feedback from the external cavity is wavelength dispersive This can be achieved by the use of a diffraction grating or a frequency selective filter The grating has the added advantage that it allows the wavelength to be tuned over a considerable range (~50nm) by rotating the grating Tunability can also be achieved by changing the cavity length This can be achieved either thermally, in which case a change in temperature changes the RI and so the optical length, or electronically, usually by the use of a piezoelectric transducer

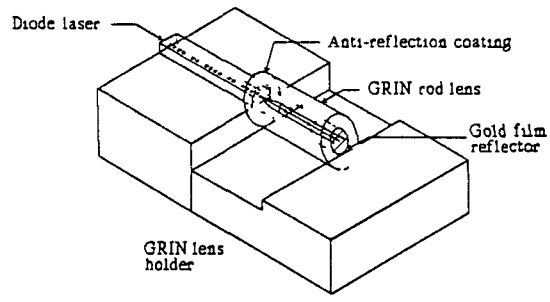

Figure 1.10: Passive coupled cavity laser.

1.6 Applications of external cavity laser diodes.

1.6.1 Communications

Current optical fibre communication trends have tended to concentrate on coherent transmission systems [6] These have shown improvements compared to standard intensity modulated direct detection systems High performance coherent optical fibre systems require narrow linewidth laser transmitters to realise the full benefits of coherent detection Linewidth requirements have been discussed previously [7] and a

Table 1: Coherent system linewidth requirements [After Ref.7].

Modulation	Demodulation		Linewidth to bit rate ratio	Suitable Lasers
	HET	HOM		
ASK, FSK, PSK	SYNC	YES	<0 1%	Gas and Ext-Cav
DPSK	DELAY	NO	<0 3%	Gas and Ext-Cav
ASK, FSK	NON-SYNC	NO	<20%	Gas and Ext-Cav and DFB

summary is presented in Table 1. Work now centres around the 1.55μm, low fibre attenuation region. Presently available 1.55μm semiconductor lasers do not themselves possess sufficient phase coherence for such applications unless external line narrowing techniques are used. The external cavity is just such a technique. Wyatt & Devlin [5] have demonstrated a linewidth reduction from 1GHz to 10kHz by the use of an external cavity, thus enabling the evaluation of a coherent optical communication system to be performed.

1.6.2 Photoluminescence excitation spectroscopy.

Optronics Ireland at Dublin City University is primarily concerned with the characterisation of III-V semiconductor materials by photoluminescence techniques. A complementary technique useful for determining weak absorption, or absorption in a thin layer on a heavily absorbing substrate, is photo-luminescence excitation spectroscopy, (PLE). The energy level diagram for PLE is shown in Figure 1.11. If the absorption process creates an excited state which can decay by photon emission of a different (lower) energy, measurement of the luminescence as a function of the energy of the excitation source can be much more sensitive than measuring a very small change in transmission. A tunable laser is an ideal candidate for such studies. In particular an external cavity diode laser is especially useful due to the linewidth narrowing which occurs. Furthermore several different diodes can be used depending on the wavelength range of interest.

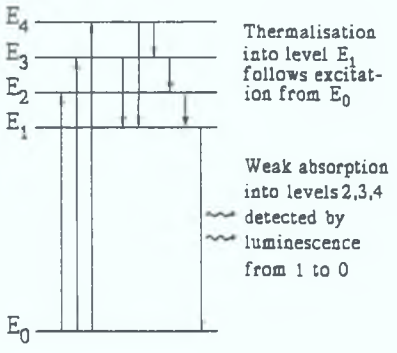

Figure 1.11: Energy level diagram for PLE.

1.6.3 Sensor devices.

External cavity systems have also found application as sensor devices [8]. These sensors consist of a laser diode tightly coupled to an external reflector, with the cavity length much shorter than the device length. The presence of this reflector creates a standing wave which alters the effective facet reflectivity of the laser diode source.

A slight change in the position of the external reflector alters the phase of the light reflected back into the laser chip This varies the effective facet reflectivity and therefore the output intensity Several sensor configurations have been designed around the external cavity

Acoustic sensor - by using a thin, pliable glass membrane either coated or uncoated, as an external resonator, an acoustic pressure wave modulates the reflector

Magnetic sensor - the reflector is attached to an element whose magnetic properties are such that a magnetic field displaces the reflector with a displacement proportional to the magnetic field strength

Current sensor - similar to the magnetic sensor It relies on the magnetic field associated with the current flowing in a wire to displace a magnetic reflector

External cavity configurations have also been used to tune to wavelengths important for sensing applications

Gas Sensor - External cavity systems have also found applications as sources for hydrocarbon gas sensors Methane, for example, exhibits a weak overtone absorption at 1 33μm and a strong overtone absorption at 1 66μm Laser diodes emitting at 1 66μm cannot be fabricated using standard techniques Work is currently in progress [9] in the fabrication of strained layer lasers designed to emit at this wavelength However, laser diodes emitting at 1 64μm could be tuned, using external cavity techniques, to emit at 1 66μm These are of considerable use in the area of methane sensing

1.7 Conclusion

This chapter has provided a general introduction to the area of semiconductor diode lasers The lasing process for these devices has been discussed and found to offer a versatility which cannot be obtained with conventional solid state or gas lasers The concept of operating laser diodes in external cavities has been addressed External cavity schemes, with both active and passive cavities have been presented Several quantities of importance in any further discussions about laser diodes, either operated in isolation, or in external cavity configurations, were introduced, namely

Threshold current The drive current at which the stimulated emission process becomes the dominant form of radiative decay

LI curve This is a plot of the variation of the output light intensity (L) against drive

current (I) Through this curve the threshold current can be found The slope of the LI curve indicates the efficiency of the lasing process for that cavity configuration, showing as it does the light output / mA value

Longitudinal mode Longitudinal modes are the different wavelengths that satisfy the Fabry Perot condition for the cavity Diode lasers, especially when operated at drive currents only slightly above threshold exhibit strong multimode behaviour, as was shown in Figure 1 4 However, when operated in an external cavity this multimode behaviour collapses to a predominantly single mode operation

The applications of these devices in the areas of communications, spectroscopy and sensors has been briefly reviewed

References.

1 Agrawal, G P and Dutta, N K *Long Wavelength Semiconductor Lasers* New York Press, 1986

2 Hsieh, J.J , Rossi, J A and Donnelly, J P *Appl Phys Letters* 28, 709, 1976

3 Hall, R N , Fenner, G E , Kingsley, J D , Soltis, T.J and Carlson, R O *Phys Rev Letters* 9, 366, 1962

4 Kogelnik, H and Shank, C V *Appl Phys Letters* 18, 152, 1971

5 Wyatt, R and Devlin, W.J *Electron Lett* **19**, No 3, 113, Feb 1983

6 Wyatt, R , Cameron, K H and Matthews, M R *Br Telecom Technol J* **3**, No 3, Oct 1985

7 Hodgkinson, T G , Smith, D W , Wyatt, R and Malyon, D J *Br Telecom Technol J* 3, No 3, Oct 1985

8 Miles, R O , Dandridge, A Tueton, A B and Giallorenzi, T G *J Lightwave Technol* **LT-1**, No 1, March 1983

9 O'Reilly, E P , *Semicond Sci Technol* **4**, 121, 1989

Chapter 2: Theory of external cavity laser diodes.

2.0 Introduction.

In this chapter the single mode rate equations are obtained for a diode laser Expressions for the threshold current and the longitudinal mode spectrum are obtained The rate equations are then modified for the specific case of a laser operating in an external cavity The effect of the external cavity on both the threshold current and the output spectrum are investigated The chapter closes with a discussion of the linewidth reduction observed in external cavity diode lasers

2.1 The rate equations for a semiconductor laser diode.

A unified approach to discussing the static, spectral and dynamic characteristics of semiconductor lasers with regard to their dependence on various device parameters is provided by the rate equations The rate equations govern the interplay between photons and charge carriers These equations were first developed in 1960 and have been used extensively to model semiconductor lasers

The electromagnetic field inside the laser cavity satisfies Maxwell's equations So the starting point of the analysis should be the wave equation,

$$\nabla^2 \mathscr{E} - \frac{\sigma}{\varepsilon_0 c^2}\frac{\partial \mathscr{E}}{\partial t} - \frac{1}{c^2}\frac{\partial^2 \mathscr{E}}{\partial t^2} = \frac{1}{\varepsilon_0 c^2}\frac{\partial^2 \mathscr{P}}{\partial t^2} \qquad \textbf{Eqn: 2.1}$$

where,

$\mathscr{E}$ = electric field vector

σ = medium conductivity

ε_0 = vacuum permittivity

c = velocity of light

$\mathscr{P}$ = induced electric polarisation

However considerable simplification occurs if it is assumed that the material response is instantaneous and that the induced polarisation, ($\mathscr{P}$), is directly proportional to even a time varying electric field, ($\mathscr{E}$) The wave equation then becomes,

$$\nabla^2 \mathscr{E} - \frac{1}{c^2}\frac{\partial^2}{\partial t^2}(\varepsilon \mathscr{E}) = 0 \qquad \textbf{Eqn: 2.2}$$

where ε is the dielectric constant and includes the loss term associated with the

medium conductivity, σ

A solution to the wave equation is given by,

$$\mathcal{E}_{(x,y,z,t)} = \frac{1}{2}\hat{X}\psi_{(x)}\phi_{(y)}\sum_{j}\sin(k_j z)\exp^{-i\omega_j t} + c.c \qquad \textbf{Eqn: 2.3}$$

This equation has assumed that the laser outputs a single lateral and transverse mode whose field profiles are given by $\psi_{(x)}$ and $\phi_{(y)}$ respectively In addition, the sinusoidal variation of the optical field in the z direction assumes facets of high reflectivities Although this is arguable in the case of a semiconductor laser, (R≈32%), its use is essential in order to avoid complicated boundary value problems and it does not introduce significant errors in the above threshold case [1] The subscript j in equation 2 3 denotes the j^{th} mode, since the cavity can support many longitudinal modes

The wave number k_j is given by,

$$k_j = \frac{\mu\Omega_j}{c} = \frac{m_j\pi c}{L} \qquad \textbf{Eqn: 2.4}$$

where Ω_j is the cavity resonance frequency = $2\pi\nu_j$, L is the cavity length, m is an integer

For simplicity consider the case of a single longitudinal mode By substituting equation 2 4 into equation 2 2, and, assuming that $E_{(t)}$ varies slowly, integrating over the entire range of x and y it can be shown that [2],

$$\frac{2i\omega}{c^2}\left[\langle\varepsilon\rangle + \frac{\omega}{2}\frac{\partial\langle\varepsilon\rangle}{\partial\omega}\right]\frac{dE}{dt} + \left[\frac{\omega^2}{c^2}\langle\varepsilon\rangle - k^2\right]E = 0 \qquad \textbf{Eqn: 2.5}$$

where $\langle\varepsilon\rangle$ is the spatially averaged dielectric constant

Note that the second term in equation 2 5 takes into account the dispersive nature of the semiconductor material It can be shown, [2], that $\langle\varepsilon\rangle$ approximately equals the effective dielectric constant of the material and may be written as,

$$\langle\varepsilon\rangle \approx \bar{\mu} + 2\Gamma\bar{\mu}\Delta\mu_p + i\bar{\mu}\bar{\alpha}/k_0 \qquad \textbf{Eqn: 2.6}$$

where $k_0 = \omega/c$ and Γ is the confinement factor, which accounts for the reduction in gain brought about by spreading of the optical mode beyond the active layer, it represents the fraction of the mode energy contained in the active region, $\Delta\mu_p$ is the change induced in the refractive index due to the presence of charge carriers, $\bar{\mu}$ is the mode index and $\bar{\alpha}$ is the mode absorption coefficient given by,

$$\bar{\alpha} = -\Gamma g + \alpha_{int} + \alpha_m \qquad \textbf{Eqn: 2.7}$$

where g is the gain of the active region, α_{int} is the internal losses due to recombination mechanisms which do not contribute to the lasing mode, α_m is the facet loss and is given by,

$$\alpha_m = \frac{1}{2L} \ln\left[\frac{1}{R_1 R_2}\right] \qquad \textbf{Eqn: 2.8}$$

where R_1 and R_2 are the facet reflectivities

Substituting equation 2 6 into 2 5 and using, $k = \bar{\mu}\,\Omega / c$, $(\omega^2 - \Omega^2) \approx 2\,\omega(\omega - \Omega)$ and $\langle \varepsilon \rangle \approx \bar{\mu}^2$, yields,

$$\frac{dE}{dt} = \frac{\imath \bar{\mu}}{\mu_g}(\omega - \Omega)E + \frac{\imath \omega}{\mu_g}(\Gamma \Delta\mu_p + \imath\alpha / 2k_0) \qquad \textbf{Eqn:2.9}$$

where μ_g is the group index corresponding to the mode index of $\bar{\mu}$

By separating equation 2 9 into its real and imaginary parts the following amplitude and phase rate equations are obtained,

$$\frac{dA}{dt} = \frac{1}{2} v_g \left[\Gamma g - (\alpha_{int} + \alpha_m)\right] A \qquad \textbf{Eqn: 2.10}$$

$$\frac{d\phi}{dt} = -\frac{\bar{\mu}}{\mu_p}(\omega - \Omega) - \frac{\omega}{\mu_g}\Gamma \Delta\mu_p \qquad \textbf{Eqn: 2.11}$$

where $v_g = c / \mu_g$ and $\bar{\alpha}$ has been eliminated using equation 2 7

Equation 2 10 could have been written directly since it simply states that the rate of amplitude growth is equal to the gain minus the loss Equation 2 11, which follows self consistently with 2 10, shows that the change in refractive index due to the charge carriers affects the lasing frequency ω

Equation 2 10 is usually written in terms of photon number, P, using

$$P = \frac{\varepsilon_0 \bar{\mu} \mu_0}{2\hbar\omega} \int (\mathcal{E})^2 dV \qquad \textbf{Eqn: 2.12}$$

where $\hbar\omega$ is the photon energy, and V the active volume Since $P \propto A^2$, then,

$$\frac{dP}{dt} = (G - \gamma)P + R_{sp} \qquad \textbf{Eqn: 2.13}$$

where $G = \Gamma v_g g$ is the net rate of stimulated emission, and

$$\gamma = v_g(\alpha_m - \alpha_{int}) = \tau_p^{-1} \qquad \textbf{Eqn: 2.14}$$

is the photon decay rate which is used to define the photon lifetime, τ_p, in the cavity R_{sp} takes into account the rate at which spontaneously emitted photons are added to the lasing photon population

Defining a parameter, β_c, called the linewidth enhancement factor, [2], such that

$$\Delta\mu_p = -\left(\frac{\beta_c}{2k_0}\right)\Delta g \qquad \textbf{Eqn: 2.15}$$

equation 2 10 then becomes

$$\frac{d\phi}{dt} = -\frac{\bar{\mu}}{\mu_g}(\omega - \Omega) + \frac{1}{2}\beta_c(G - \gamma) \qquad \textbf{Eqn: 2.16}$$

Equation 2 16 shows that when the gain changes from its threshold value the phase shifts as well This is understandable since a gain change is always accompanied by a change in refractive index This change in index changes the lasing frequency

The gain G is known in terms of the carrier density, n If the number of carriers in the active layer is defined as

$$N = \int n\,dV = nV \qquad \textbf{Eqn: 2.17}$$

where $V = L\,w\,d$ and is the volume of the active area (length L, width w, thickness d)

The carrier rate equation can be shown to be [2],

$$\frac{dN}{dt} = \frac{I}{q} - \gamma_e N - GP \qquad \textbf{Eqn: 2.18}$$

where $I = w\,L\,J$, with J being the current density in the active layer, q the electronic charge and

$$\gamma_e = (A_{nr} + Bn + Cn^2) = \tau_e^{-1} \qquad \textbf{Eqn: 2.19}$$

is the carrier recombination rate that defines the carrier lifetime τ_e The terms A_{nr}, B and C are the various recombination mechanisms, B is the radiative recombination rate, C is the recombination rate due to Auger processes and A_{nr} accounts for all other non-radiative recombination processes GP is due to stimulated recombination which leads to a non-linear coupling between photons and charge carriers

To complete the rate equation description an expression for R_{sp}, appearing in equation 2 13, is required If it is assumed that a fraction β_{sp} of spontaneously emitted photons goes into the lasing mode, R_{sp} is given by

where $\eta_{sp} = B\,n / \gamma_e$ is the spontaneous quantum efficiency

$$R_{sp} = \beta_{sp}\eta_{sp}\gamma_e N \qquad \textbf{Eqn: 2.20}$$

Equations 2 13, 2 16 and 2 18 are the single mode rate equations that will be used in this chapter to describe the behaviour of the laser in the external cavity However for a discussion of the modal phenomena which occur these equations must be generalised to include the number of possible longitudinal modes for which G is positive This depends on the width of the gain spectrum and the frequency between modes

The multimode rate equations are,

$$\frac{dP_m}{dt} = (G_m - \gamma_m)P_m + R_{sp}(\omega_m) \qquad \textbf{Eqn: 2.21}$$

$$\frac{dN}{dt} = \left[\frac{I}{q} - \gamma_c N\right] - \sum_m G_m P_m \qquad \textbf{Eqn: 2.22}$$

where P_m represents the photon population of the m^{th} longitudinal mode oscillating at a frequency ω_m $G_m = G(\omega_m)$ is the mode gain and γ_m is the mode loss

A quantity of practical interest is the output power emitted from each facet This is linearly related to the photon population and is given by,

$$P_m^{out} = \frac{1}{2}\hbar\omega v_g \alpha_m P_m \qquad \textbf{Eqn: 2.23}$$

For ease of reference Table A 1 in Appendix A gives typical parameter values for a 1 3μm buried heterostructure laser similar to those used in this work

The steady state response of a laser may be obtained by setting the time derivatives of the rate equations to zero Two steady state features of importance are the light-current (LI) curve and the longitudinal mode spectrum

2.2 Light-current curve.

Equation 2 13 gives the photon number, P as

$$P = \frac{R_{sp}}{(\gamma - G)} \qquad \textbf{Eqn: 2.24}$$

The LI curve is obtained by substituting equation 2 24 into 2 18, where $dN/dt = 0$ for steady state This yields,

$$\gamma_e(N)N + R_{sp}(N)\left[\frac{G}{\gamma - G}\right] = \frac{I}{q} \qquad \textbf{Eqn: 2.25}$$

which can be used to obtain N for a given I if the functional dependence of $G(N)$ is

known The photon number P is then obtained using equation 2 24 The output power is linearly related to P as given by equation 2 23 The quantity of interest is the threshold current, I_{th}, ie the point at which stimulated emission has taken over from spontaneous emission In the presence of spontaneous emission the threshold is not sharply defined, but depends on β_{sp}, the spontaneous emission factor The threshold transition becomes less severe with increasing spontaneous emission It is customary to define I_{th} in the limiting case when $\beta_{sp} = 0$ In this case

$$I_{th} = q\gamma_e(N_{th})N_{th} \qquad \textbf{Eqn: 2.26}$$

where N_{th} is the number of carriers at threshold and γ_e is expressed as a function of N_{th} It should be stressed that equation 2 26 expresses the current through the active region In practice the threshold current is slightly higher due to current leakage outside the active layer

2.3 Longitudinal mode spectrum.

The output spectrum of a semiconductor laser shows the presence of several longitudinal modes due to the Fabry-Perot nature of the device However the relative powers of those modes vary with drive current I The rate equations can be used to calculate the number of these modes and their relative intensities

In order to solve the multimode rate equations 2 22 and 2 23, the gain spectrum must be known A simple approximation is that [2]

$$G_{(\omega)} = G_0\left[1 - \left(\frac{\omega - \omega_0}{\Delta\omega_g}\right)^2\right] \qquad \textbf{Eqn: 2.27}$$

where ω_0 is the frequency at which the gain is a minimum G_0, $\Delta\omega_g$ is the spread of frequency over which the gain is non zero Using this the modal gain is approximated by

$$G_m = G_0\left[1 - (m/M)^2\right] \qquad \textbf{Eqn: 2.28}$$

where m is an integer which varies from $-M$ to $+M$

Assuming that all modes have the same loss $\gamma = \tau_p^{-1}$ (τ_p^{-1} is the photon lifetime), the photon number can be given by

$$P_m = \frac{R_{sp}(\omega_m)}{\gamma - G_m} \equiv \frac{R_{sp}(\omega_m)}{\gamma}\left[\sigma + (m/M)^2\right]^{-1} \qquad \textbf{Eqn: 2.29}$$

where

$$\sigma = \frac{R_{sp}(\omega_0)}{\gamma P_0} \qquad \textbf{Eqn: 2.30}$$

Equations 2.29, 2.28 and 2.23 can then be used to obtain the steady state carrier number N which in turn determines G_m and the steady state photon population P_m for each current value. It is found that below threshold the power in all modes increases with an increase in current. However above threshold the power in the main mode continues to increase while the power of the side modes saturates. The level at which this saturation occurs is found to depend on the spontaneous emission factor B_{sp}.

A measure of the spectral purity of the laser is the mode suppression ratio (MSR) which is defined as the ratio of the power in the main mode to that of the next most intense side mode. Mathematically,

$$MSR = \frac{P_0}{P_1} = 1 + \frac{P_0}{\tau_p R_{sp}}\left(\frac{\Delta\omega_L}{\Delta\omega_g}\right)^2 \qquad \textbf{Eqn: 2.31}$$

where $\Delta\omega_L$ is the longitudinal mode spacing. The term, single mode operation, implies a large value of MSR. However the exact value above which a laser qualifies as single mode is a matter of definition. In practice a value of 10 is often used. The total power emitted by a multimode laser may be obtained by summing over all the modes [3] ie.

$$P_T = \sum_n P_m = \frac{R_{sp}(\omega_0)}{\gamma\,\sigma^{1/2}}\,\pi M \coth(\pi M \sigma^{1/2}) \qquad \textbf{Eqn: 2.32}$$

This analysis has shown that the multimode characteristics can be described in terms of two dimensionless parameters, σ and M. The figure $2M+1$ corresponds to the total number of longitudinal modes that fit within the gain spectrum and experience gain. The parameter σ is a measure of how closely the peak gain approaches the total cavity loss. It decreases with increasing power. In this approach the multimode operation has been attributed to spontaneous emission. The laser behaves as a regenerative noise amplifier in which all modes with positive round trip gain undergo amplification. On reaching threshold the gain is approximately clamped and the power in the side modes

saturates The MSR then increases with increasing power In practice, with an increase in laser power, spectral and spatial hole burning start to influence the output spectrum Spatial hole burning is a result of the standing wave nature of the optical mode and is known to lead to multimode operation [4], with increasing side mode power above a critical main mode power value

Spectral hole burning is related to gain boundary mechanisms At high powers this leads to a shifting of the main mode towards longer wavelengths [5]

2.4 Modified rate equations for external cavity lasers.

In order to analyse the external cavity it is necessary to consider both the gain and loss in the two cavities while taking into account their mutual optical feedback Within an external cavity the facet loss becomes wavelength dependant due to the FP modes established

A general analysis of external cavity semiconductor lasers is extremely complicated, therefore several simplifying assumptions are made It is assumed that the field distributions associated with the lateral and transverse modes are unaffected by coupling to the cavity and that only axial propagation need be considered This reduces the problem to one dimension Note however, that coupling depends on the mode-width and that mode conversion losses occur due to the nature of the cavity The first step in the analysis is to determine the extent of coupling between the two cavities In the case of a semiconductor laser coupled to an external mirror where R is the facet reflectivity into the cavity it is useful to define a complex coupling parameter $\check{C}$, such that

$$\check{C} = C\exp(\iota\theta) \qquad \textbf{Eqn: 2.33}$$

where

$$C = \left[1 - R^2\right]^{1/2}/R \qquad \textbf{Eqn: 2.34}$$

governs the strength of the coupling and

$$\theta = \frac{\pi}{2} \qquad \textbf{Eqn: 2.35}$$

is the coupling phase

Although the multimode rate equations should be considered, the analysis is simplified

considerably by using the single mode equations This is justified since, for this application, the device must behave as a single mode device A generalisation of the rate equations developed in Section 2 1 can be carried out by noting that on every reflection a fraction of the field in the external cavity is coupled into the active region Since this fraction is complex, both the power and the phase are affected Noting this, the generalised rate equations are found to be, [6],

$$\frac{dP_j}{dt} = (G_j - \gamma_j)P_j + R_{sp}(N_j) + \varkappa_j \cos(\theta \pm \phi) \qquad \textbf{Eqn: 2.36}$$

$$\frac{dN}{dt} = \frac{I_j}{q} - \gamma_e(N_j)N_j - G_j P_j \qquad \textbf{Eqn: 2.37}$$

$$\frac{d\phi_j}{dt} = -\frac{\mu_j}{\mu_{gj}}(\omega - \Omega_j) + \tfrac{1}{2}\beta_c(G_j - \gamma_j) + \frac{\varkappa_j}{2P_j}\sin(\theta \pm \phi) \qquad \textbf{Eqn: 2.38}$$

where ϕ is the relative phase between the two cavities The feedback rate, $\varkappa_j$, is the rate at which photons are added back into the cavity, and is given by [6]

$$\varkappa_j = \frac{c}{n_j L_j}(P_1 P_2)^{1/2} C \qquad \textbf{Eqn: 2.39}$$

It is important to note that if the feedback rate $\varkappa_j = 0$ then the modified rate equations reduce to the single mode rate equations 2 13, 2 18, 2 16

The external cavity rate equations give a full description of the behaviour of the diode in the external cavity This analysis is extremely complicated Therefore the remainder of the chapter will concentrate on a discussion of the features of external cavity behaviour that are of interest in this project. These are, the light-current characteristics, the output spectrum and the laser linewidth

2.5 Light-current characteristics.

It is useful at this point to introduce the concept of an effective reflectivity, R_{eff} The effects of the external cavity on the FP mode of the active laser can be treated by an effective reflectivity for the laser facet facing the external cavity [7] It is obvious that R_{eff} would be strongly proportional to the coupling strength C The stronger the coupling between the two cavities, the higher R_{eff} will be Recalling equation 2 34 note that

$$C = \left[1 - R^2\right]^{1/2}/R \qquad \textbf{Eqn: 2.40}$$

This shows that strong coupling is dependent on weak facet reflectivity Therefore in order to increase coupling with the external cavity the facet facing the cavity should be antireflection, (AR), coated

The threshold current, as outlined in Section 2 2, is given by

$$I_{th} = q\gamma_e(N_{th})N_{th} \qquad \textbf{Eqn: 2.41}$$

where N_{th} is the carrier population at threshold and corresponds to the condition $G = \gamma$, i e gain = loss Equation 2 14 defines γ *as*

$$\gamma = v_g(\alpha_m - \alpha_{int}) \qquad \textbf{Eqn: 2.42}$$

Also, modifying equation 2 8 to take account of the effective reflectivity then

$$\alpha_m = \frac{1}{2L}\ln\left[\frac{1}{R_1 R_{eff}}\right] \qquad \textbf{Eqn: 2.43}$$

It is obvious therefore that in the case of a semiconductor laser operating in an external cavity the threshold current depends on the strength of the coupling C Strong coupling reduces I_{th} by increasing R_{eff}, thereby reducing the cavity loss The threshold reduction expressed here is demonstrated by the external cavity and the results are presented in Chapter 4

2.6 External cavity longitudinal mode spectrum.

Fleming and Mooradian [8] have indicated that for a given drive current the external cavity laser generally has lower power output than the solitary laser However whereas the output of the solitary laser is multimode, the external cavity operates in a single longitudinal mode This single mode operation is not simply a result of wavelength selectivity provided by the diffraction grating used as the reflector Results with plane mirror reflectors have also shown stable single mode operation However the external cavity presented in this work makes use of a diffraction gratmg as the reflector

Mode discrimination is found to be strongly dependant on the phase, θ, of the coupled light In the case of a plane mirror reflector, i e where the laser-air interface is the coupling element, the phase is found to be $\pi/2$ This is found to be the optimum condition for maximum mode discrimination both theoretically [9] and experimentally

[10] The results that are presented in Chapter 4 for the external cavity described in this work will be seen to also show good mode descrimination

2.7 Linewidth.

In the previous discussions laser power and frequency were assumed to remain constant once the steady state has been achieved In practice however, laser outputs exhibit intensity as well as phase fluctuations The origin of these fluctuations lies in the quantum nature of the lasing process itself and is beyond the scope of this work In general however, the intensity noise peaks near the laser threshold and then decreases rapidly as the drive current is increased Phase noise is manifested as a broadening of each longitudinal mode and is responsible for the observed linewidth One of the predominant features of the external cavity output spectrum is its narrow linewidth It is therefore important that this linewidth reduction be quantifiable for the cavity presented in this work Due to the length of the new optical cavity the spontaneous-recombination phase fluctuations in the laser linewidth can be dramatically reduced The reason for this is as follows the number of spontaneous photons above threshold remains constant whereas the number of stimulated photons above threshold continues to rise Therefore the spontaneous phase fluctuations m the laser frequency could be expected to be inversely proportional to the stimulated power The full width half maximum (FWHM) of the power spectrum is given by the Schawlow-Townes formula [11]

$$2\Gamma_m = \frac{\pi h \nu_m (\Delta\nu_c)^2}{P_m} n_{sp} \qquad \textbf{Eqn: 2.44}$$

where $\Delta\nu_c$ is the FWHM of the FP cavity, P_m is the power of the mode, n_{sp} is the number of spontaneous photons in the mode (Note above threshold n_{sp} approaches unity)

$\Delta\nu_c$ is related to the photon lifetime τ_p and therefore, to the cavity loss For a diode operating outside an external cavity the cavity bandwidth is [12]

$$\Delta\nu_{cSD} = \frac{1}{2\pi}\frac{c}{nl}\left(\alpha l - \ln\sqrt{R_1 R_2}\right) \qquad \textbf{Eqn: 2.45}$$

where n is the refractive index of the active region, R_1 and R_2 are the facet

reflectivities, l is the length of the active layer and α is the photon loss This equation must be modified in order to characterise the diode under external cavity operation, where the photon lifetime is significantly longer due to loss-free propagation over a distance $L >> nl$

$$\Delta\nu_{cEC} = \frac{1}{2\pi}\frac{c}{nl+L}\left(\alpha l - \ln\sqrt{R_g T^4}\right) \qquad \textbf{Eqn: 2.46}$$

In this case L corresponds to the length of the external cavity T is a measure of the coupling efficiency into the active layer and takes into account the transmission characteristics of the collimation optics R_g is the reflectivity of the grating
Wyatt and Devlin, [13], have used the above approach to determine the linewidth of a 1 5μm InGaAsP-InP laser operating in an external cavity similar to that presented here They found good agreement between predicted linewidth and that measured experimentally using heterodyne beat frequency measurements A reduction of four orders of magnitude from 1GHz to 10kHz (measured) was demonstrated by using the diode in an external cavity configuration

2.8 Conclusion.

In this chapter the behaviour of laser diodes when operated in an external cavity configuration has been examined The observed reduction in threshold current has been explained in terms of the effective reflectivity of the cavity Single mode operation ot the laser in an external cavity has been seen to be due to the interaction between the cavity loss profile and the gain roll-off of the active medium In Chapter 3 the experimental setup of a practical external cavity diode laser using a 1 3μm InGaAsP-InP laser chip as the active medium is described

References:

1 Lau, K Y , and Yariv, A, *Semiconductors and semimetals* 22, Part B, ed W T Tsang, New York, Academic Press, 1985

2 Agrawal, G P and Dutta, N K , *Long wavelength semiconductor lasers* New York Press, 1986

3 Casperson, L W *J Appl Physics* **46**, 5794, 1984

4 Statz, H , Tang, C L , Lavine, J M , *J Appl Phys* **35**, 2851, 1964

5 Zee, B , *IEEE J Quantum Electron* **QE-14**, 727, 1978

6 Agrawal, G P *IEEE J Quantum Electron* **QE-21**, 255, 1985

7 Choi, H K , Chen, K L and Wang, S *IEEE J Quantum Electron* **QE-20**, 385, 1984

8 Fleming, M W , and Mooradian, A , *IEEE J Quantum Electron* **QE-17**, 44 1981

9 Marcuse, D and Lee, T P , *IEEE J Quantum Electron* **QE-20**, 166, 1984

10 Preston, K R , Woollard, K C , and Cameron, K H , *Electron Lett* 17, 931, 1981

11 Lax, M , *Phys of Quantum Electronics* New York, M^{c} Graw Hill 735-747

12 Yariv, A , *Quantum Electronics* 2nd ed New York, Wiley, 1975

13 Wyatt, R and Devlin, W J *Electron Lett* **19**, No 3, 113, Feb 1983

Chapter 3: Experimental Setup

3.0 Introduction.

Details of the design and construction of the external cavity are provided in this chapter The cavity, illustrated schematically in Figure 3 1, is discussed in terms of its electronic, thermal, optical and mechanical requirements There is also a discussion of the detection and analysis systems used in the characterisation of the device as a whole The chapter commences with a description of the laser diode itself and the system requirements necessary for its safe operation

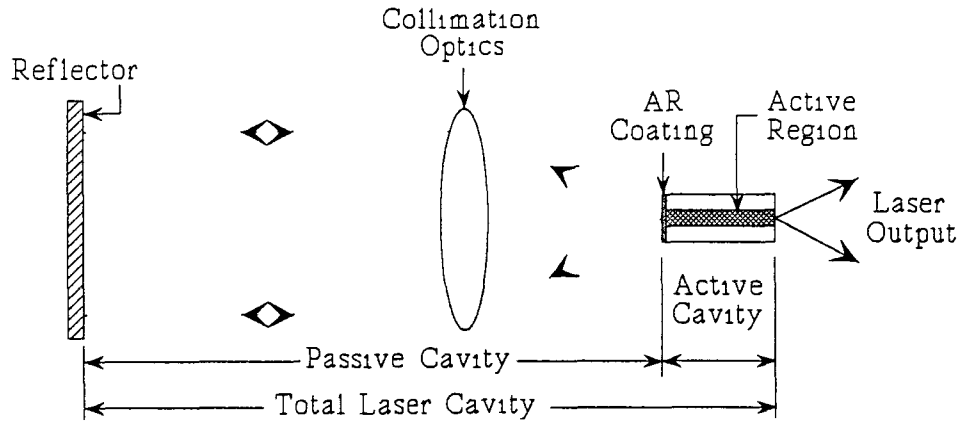

Figure 3.1: A generalised external cavity laser diode.

3.1 The laser diode.

The laser diodes used throughout this project were all planar buried heterostructure index guided devices The active layer is InGaAsP lattice matched to an InP substrate, designed to emit nominally at 1 3μm in the near infra-red These devices were supplied by British Telecom Research Laboratories, (BTRL) Ipswich U K The active region of the device is approximately 100μm long, 2μm in width and 0 5μm in thickness This small cross sectional area gives rise to a highly divergent, partially polarised output The laser chip is bonded to a pure diamond heat sink which in turn is bonded to a brass mounting stud. This is shown in Figure 3 2 Electrical connections are made via the brass stud and one of the two tags, which has a very fine wire

bonded between it and the semiconductor Although the chip is normally bonded p side down, there have been lasers supplied bonded n side down Therefore care must be taken with the polarity of the electrical connections All the lasers supplied for use in this project have had an antireflection coating (AR) applied to one output facet This is a BTRL proprietary multilayer coating which reduces the facet reflectivity and allows greater coupling of the light with the external cavity

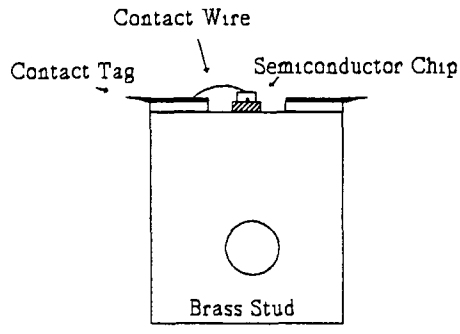

Figure 3.2: The laser stud.

3.2 Laser current source.

Before the laser can be inserted in any drive circuitry certain handling precautions must be observed

1) The laser must only be handled while wearing a grounded, conductive wrist strap
2) Only a grounded soldering iron should be used and only for the time / temperature recommended by the supplier
3) All work must be done on a conductive bench mat
4) The device must be handled with care Chip mounted diodes as used in this project have little or no mechanical protection

Obviously the ease with which laser diodes can be damaged or destroyed must be taken into consideration when a drive circuit is being designed The circuit used to drive the laser for this project is shown in Figure 3 3[1] The circuit is battery driven, thus reducing the amount of noise and keeping transient suppression requirements to a minimum The slow start section (shown here in a dashed box) delays the switch on of the circuit proper The duration of this delay, which is set by C_2 and C_3, is longer than the settling time of the voltage regulator and ensures that voltage transients, due

[1] PCB foil and parts list for all circuits are provided in Appendix B

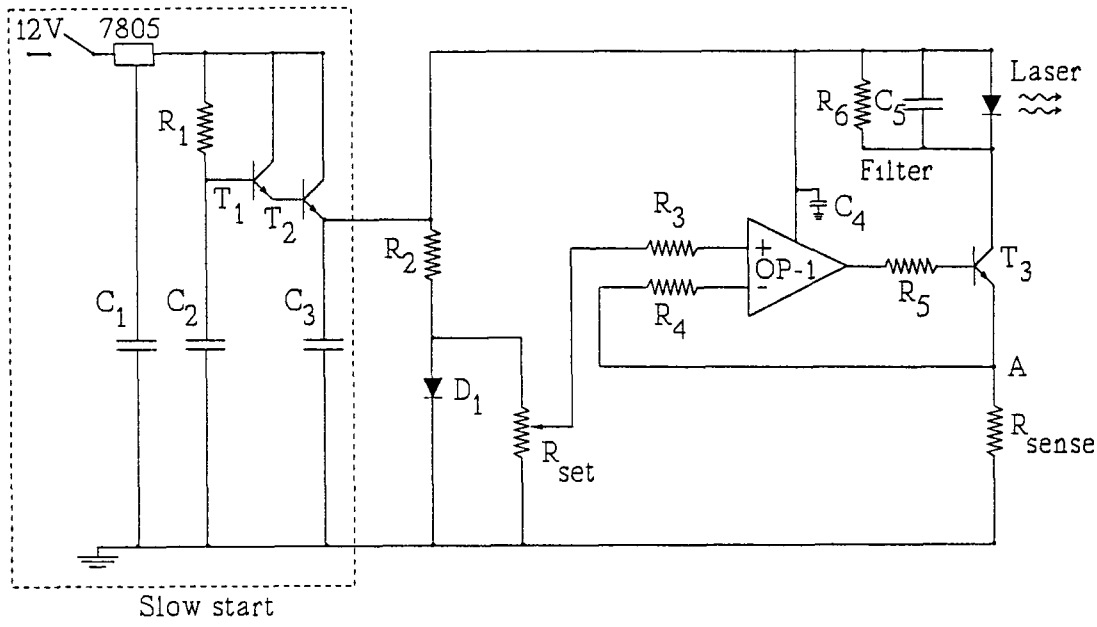

Figure 3.3. The laser current supply circuit. Component values are given in Appendix B.

to this regulator, and also switching surges, do not reach the laser The circuit itself is an Automatic Current Control, (ACC), in which the current to the laser is controlled by the 10kΩ potentiometer For safe operation this is always turned to minimum (anticlockwise) before the laser is turned on or off The operation of the circuit is as follows with the current to the laser set, the output of the op-amp is such that the voltage at point A is equal to the set voltage Any change in the current through the laser will cause a corresponding change in the voltage at point A This causes an imbalance between the two inputs of the op-amp, which is then compensated for at the output, thus returning the current to the set value The purpose of the resistor and capacitor at both the laser head and the op-amp output is to slow the circuit response to sudden changes The current is indicated by an LCD panel meter in series with the laser Cross talk of the screen update frequency to the laser power lines has been filtered out to prevent damage to the laser The power supply lines to the laser head have been shielded to reduce pick-up Further RC filters have been added to decrease the remaining noise levels The circuit provides current from 0-110mA with a measured peak to peak drift value of < 0.2mV/hr, which corresponds to 0.012 ppm per hour drift in the drive current This is considered adequate for this application

3.3 Temperature control.

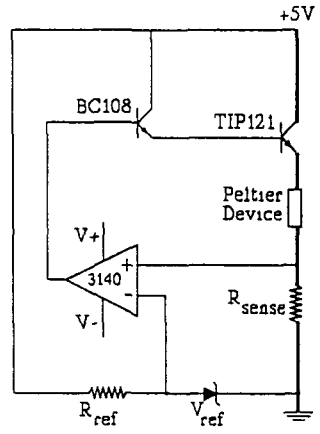

Figure 3.4: Peltier current supply.

Since variation in temperature is a mechanism by which the output of the laser diode may be tuned, it is obvious that control of device temperature is critical for stable operation at a single wavelength The thermal control of the laser diode is based around a THOR Cryogenics E3010 temperature controller This instrument is designed to control accurately the temperature of a sample to within ±0 01°C of a set value Although primarily designed for control of samples in cryogenic applications, its versatility is such that it is suitable for temperature control of the laser diode in this project Use of a Peltier effect device as a heat pump to draw both ambient, and evolved heat, away to a heatsink provides a greater degree of freedom, allowing operation above and below room temperature The circuit used to supply the Peltier device with the 1 Amp necessary is shown in Figure 3 4 The stability of the output of this circuit ensures that it does not contribute to device temperature fluctuations The reference voltage is supplied by a 1 26V temperature compensated bandgap voltage reference source The rest of the circuit is a series pass circuit with the error signal derived from the drop across the sensing resistor in the currents path to ground The high current path is shown in bold The Darlington pair serves to reduce the drive current to a few milliamps, thus allowing conventional operational ampslifiers to be used In order to reduce the effects of I^2R heating of R_{sense}, and the subsequent drift in Peltier current, R_{sense} is made up of 10 resistors operated in parallel to reduce the individual loading The thermal system is shown schematically in Figure 3 5 Heat is pumped from the diode mount to

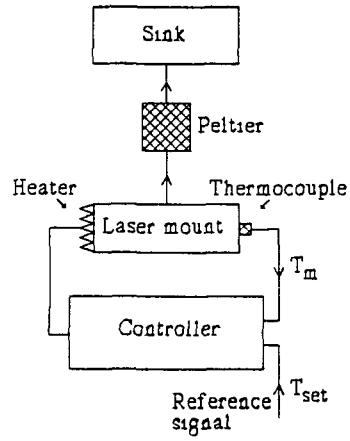

Figure 3.5: Temperature control block diagram.

the heatsink by the Peltier The temperature of the mount, T_m, is sensed by the thermocouple, and the amplified sensor output is fed to the controller This output is compared to the set voltage, corresponding to the set temperature, T_{set} Heat is supplied to the mount, by a resistive heater, according to the temperature difference $\Delta T = T_m - T_{set}$ In order to ensure optimum response without overshoot or oscillations the rate of heat supplied, Q, must be proportional to

1) The temperature difference, ΔT
2) The rate of change of this difference, $d(\Delta T) / dt$
3) The integral over time of this difference, $\int \Delta T\, dt$

These three terms are adjusted independently by the controller to match the thermal characteristics of the system To obtain the best response the derivative and integral terms must be set In order to do this the controller is operated in proportional mode only (i e no derivative or integral action) and the error monitored for increasing gain settings At a certain gain setting the temperature of the mount begins to oscillate about its set point due to the proportional action of the controller The period, (t), of this oscillation is then used to calculate values for the derivative and integral capacitors (CD and CI respectively) according to

$$CD = 6\,50\times10^{-4}\ \ t \quad (\mu F)$$

$$CI = 3\,07\times10^{3}\ \ t \quad (\mu F)$$

where the numerical constant have been provided by the manufacturer Low leakage capacitors of these values are then inserted into the slots provided at the rear of the controller Full three term PID control is then available, matched to the thermal characteristics of the laser diode mount

Error signals of $\pm 0\,1°C / hr$ have been monitored using this system, this more than satisfies the BTRL recommendation of $\pm 1°C$ for an external cavity in the present configuration [1]

3.4 Optical layout.

Figure 3 6 shows the cavity layout including an indication of the degree of freedom of each of the various components The light output from the laser is collimated from both facets This is done using two Ealing 25-0027 Infrared Achromatic microscope objectives These objectives, although designed primarily for optical fibre applications, are ideal for use in the external cavity since, in addition to their achromaticity at

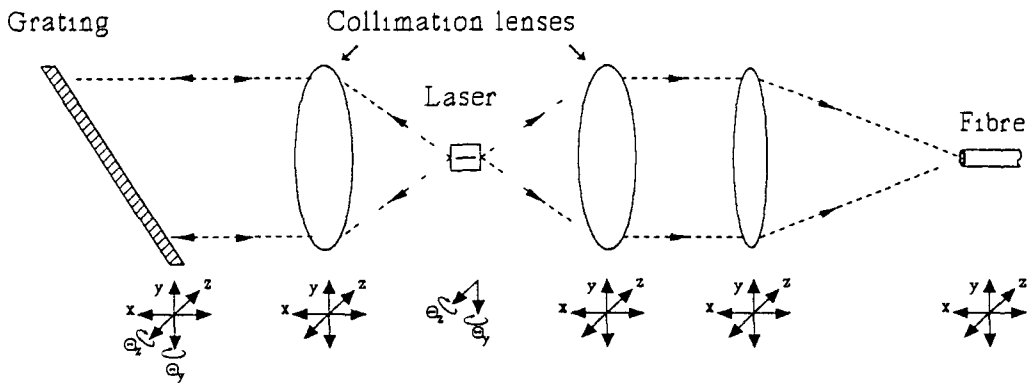

Figure 3.6 External cavity optical layout.

1 3μm , all internal optical surfaces are single layer antireflection coated This coating reduces parasitic reflections which can contribute to the formation of a multiple cavity system These objectives are large area, long working distance optics, an important feature since close access to the diode facet is difficult to achieve

The wavelength dispersive element used is a diffraction grating The collimated light from the AR coated facet is incident on this grating which has 1200 lines/mm This photoreplica grating is blazed for 1 5μm and has approximately 30% efficiency into the 1st order diffracted beam, the remaining light being lost to reflection and other orders The grating is mounted in the Littrow geometry [2] i e mounted such that the 1st order diffracted is co-axial with the incident beam and therefore retraces its path to the active region of the laser This is a common configuration for all grating tuned external cavity lasers and was first used in semiconductor laser external cavities in 1970 [3] Since the degree of dispersion is directly proportional to the number of lines of the grating illuminated [4] the importance of a large diameter collimated beam is apparent It is, however, an over simplification of the situation to assume that the final resolution depends only on that of the grating The small area of the active region acts as a resolving aperture, thus increasing the wavelength resolution In addition, several conditions must be satisfied for laser oscillation to occur at a given wavelength

(i) The Fabry-Perot condition must be satisfied for that wavelength by the cavity

(ii) The Littrow condition must be satisfied

(iii) The active medium must be able to provide gain at that wavelength

Once these conditions are fulfilled laser oscillation may be sustained

The output from the uncoated facet is fibre coupled to the detection and analysis systems The fibre used for this is Anhydride G, a Tech Optic visible-IR fibre with a 600μm core This plastic coated silica (PCS) fibre is 99 99% transmitting at 1 3μm Due to the difficulty involved in cleaving such large diameter fibres the end faces are polished to increase coupling efficiency by reducing launch losses The fibre launch stage is shown in Figure 3 7 This Martok launch stage uses a microscope objective to focus the light on to the fibre face The fibre itself is held in a v-groove and is adjustable over the plane of focus of the objective

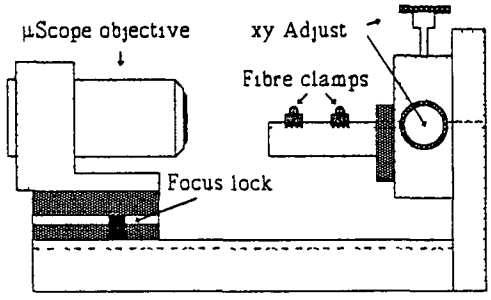

Figure 3.7: Fibre launch stage.

3.5 Mounts.

The laser diode mount is illustrated in Figure 3 8 As can be seen the laser is mounted to a copper block which houses the heater element To protect the laser in case of short circuit of the heater to the block, the laser is kept electrically isolated from the block by a thin piece of mica The good thermal conductivity of the mica ensures that the temperature control of the laser is not compromised This block is connected to the heat sink by the Peltier heat pump Thermal isolation from the sink is achieved by a layer of hard-setting epoxy resin This resin exhibits excellent thermal barrier

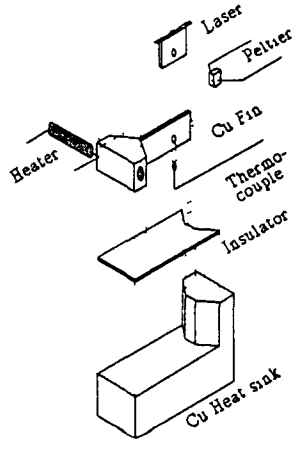

Figure 3.8: The laser mount.

characteristics This entire unit is then mounted on an optical post The design of this post allows a small degree of rotational and pitch adjustment, thus allowing the laser to be aligned along the optical axis

The collimation optics are mounted in Photon Control translation stage units allowing 3 axes of linear motion, x, y and z These stages are designed for light load (up to 30kg) applications and run on hardened ball and race track Backlash along the direction of travel has been reduced by preloading each axis This results in an improved performance for these low cost stages Each x,y,z unit is mounted on a spacer block such that the optic axis, OA, is approximately half way on the z stage travel

The grating is fitted, via an adaptor ring, to a Newport Research Corp precision gimbal optic mount This mount provides ultra stable positioning of the grating The mount has 360° coarse and ± 5° fine adjustment for both axes of rotation This mount has been fitted to a Photon Control xyz translation stage which allows the cavity length to be varied by 25mm without the need for repositioning The complete external cavity is fixed to a 3' by 1' Photon Control optical breadboard, tapped with M6 holes on a 1" grid

3.6 Drives.

It is obvious from the cavity design that specific elements have their own adjustment requirements Varying degrees of adjustment sensitivity are needed, from coarse to ultra fine To this end several different drives appear in the cavity design. For coarse adjustment of the collimation objectives standard micrometers are used on all axes These micrometers are magnetically coupled to the translation stages to minimise backlash They provide 25mm of travel for all axes and are readable to 0 01mm However for fine adjustment of the objective into the cavity itself, where high resolution positioning is required, piezo electric transducers are used These low voltage (0-150Volts) piezo give 30μm of continuous adjustment, which ensures optimum coupling both into the passive cavity and, on diffraction, into the active region of the laser These LP Piezomechanik transducers are controlled using a 3 axis voltage regulator

For adjustment of both the rotational (Θ_y) and tilt (Θ_z) axes of the grating, Newport Research Corporation differential micrometers are used These provide 13mm of

coarse adjustment readable to 0.01mm and 0.2mm of fine travel readable to 0.5μm. This allows accurate, sub arc-second adjustment of the grating orientation.

Finally, adjustment of the fibre position in the focal plane of the launch objective is made using two adjustment screws on the launch stage. Focus adjustment from this stage is crude, being achieved by sliding the objective along a track. In practice a compromise is reached using the output collimation objective.

3.7 Detection and analysis systems.

For light versus current characteristics, where spectral information is not required, the output from the cavity is monitored by a MACAM Photometrics germanium detector. Using a similar mount to that of the fibre launch stage previously discussed, the output from the fibre is focused onto this small area detector using a microscope objective. The output from this detector is fed directly to the ammeter since, due to the high intensity, amplification is unnecessary.

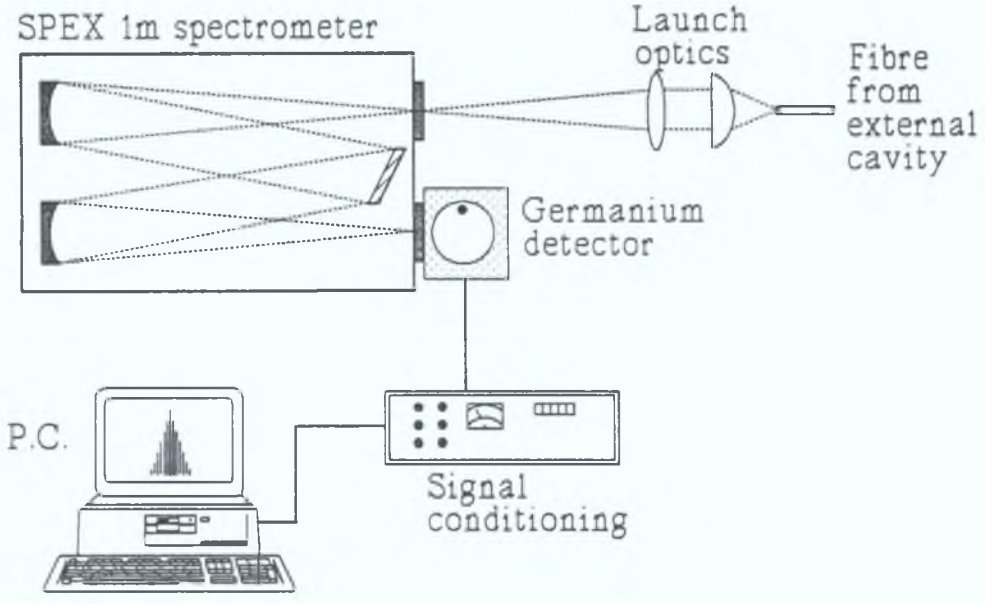

Figure 3.9: Grating spectrometer based analysis system.

Where spectral information is required the system as shown in Figure 3.9 is used. This comprises a 1m focal length SPEX monochromator fitted with an IR grating. The output from the fibre is focused on the entrance slit of this monochromator. The

spectrally resolved output is focused on a North Coast germanium detector operating at liquid nitrogen temperature The detector output is passed to conditioning electronics which can provide gain (usually set at unity due to the high intensity of the laser light) and scales the voltage range making it PC compatible The data acquisition is PC controlled with the user selecting the wavelength range, scan speed and wavelength increment between successive data points This system is primarily designed for photoluminescent (PL) studies of semiconductor samples and is therefore optimised to detect the weak light levels associated with PL work The relatively high power of the external cavity laser therefore requires either defocussing or the use of neutral density filters to reduce the power in order not to overload the detector electronics The wavelength resolution of this system is approximately 1 x 10^{-4}μm which restricts its usefulness where high resolution measurements are to be made

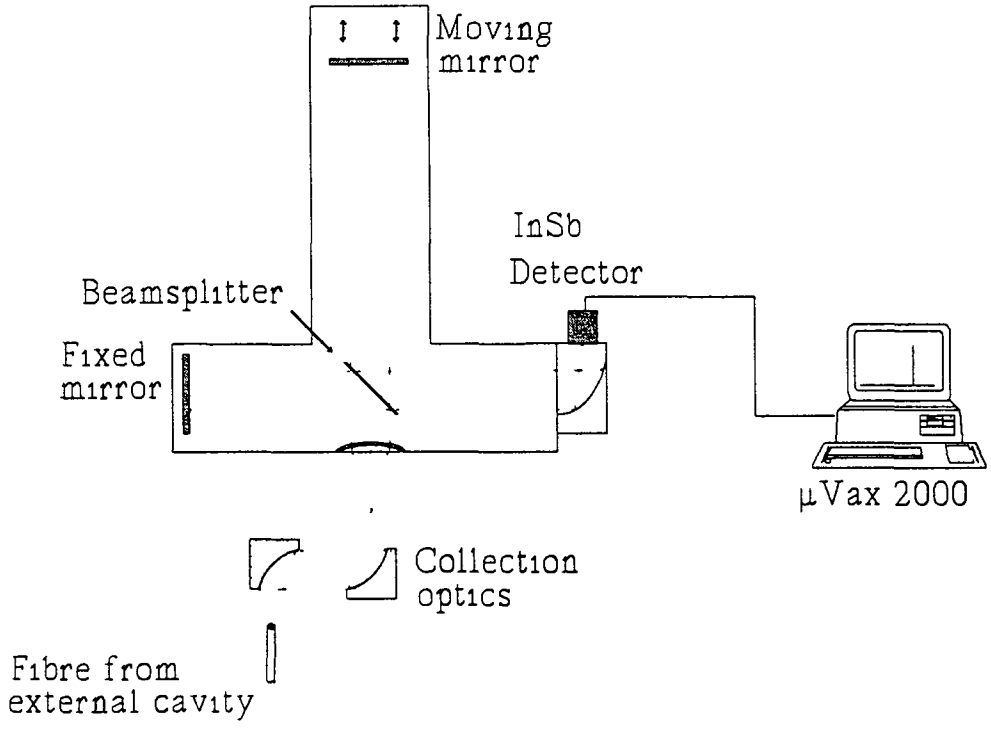

Figure 3.10: The FTIR system.

For high resolution measurements, eg linewidth, a BOMEM Fourier transform infra red spectrometer, (FTIR), is used This instrument is based around a scanning Michelson interferometer where changes in the optical path differences between the two beams give rise to intensity changes at the output This changing intensity is focused on a detector and recorded as an interferogram The Fourier transform of this

interferogram yields the spectrum The instrument is shown schematically in Figure 3 10 The resolution of the FTIR is determined by the distance over which the movable mirror is scanned For this project, a resolution of $1\ 5 \times 10^{-5}$μm was the best achievable The interferogram data is fed to the vector processor, a dedicated mathematics unit which performs the transform The resulting spectral data is then processed by a MICRO-VAX computer and the spectrum displayed on the host terminal

3.8 Conclusion.

The design and construction of the grating tunable external cavity diode laser have been discussed in this chapter Details of the laser system with regard to thermal, electronic requirements and handling techniques have been addressed The experimental systems used to characterise the performance of the external cavity laser have also been discussed The results of this characterisation are presented in the next chapter

References.

1 Sherlock, G In correspondence, BTRL, Ipswich, UK

2 Born, M and Wolf, E *Principles of Optics* Pregamon Press, 1980

3 Edmonds, H D , Smith, A W *IEEE J Quantum Electronics* **QE-6**, 356, 1970

4 Kingslake, R *Optical System Design* Academic Press, 1983

Chapter 4: Results

4.0 Introduction.

In this chapter the performance of the external cavity is evaluated The presence of optical feedback in the active region of the diode is established by the associated reduction in the device threshold current The tuning range of the cavity, both by grating rotation and by altering other diode parameters, is found The formulae developed in Chapter 2 are used to estimate the reduced laser linewidth due to cavity operation

4.1 Operation of the external cavity.

One of the desirable properties of an external cavity system is accessibility of any external cavity longitudinal mode across a broad tuning range A wide tuning range requires that the grating bandwidth be narrow in comparison to the internal mode spacing, which is typically 1nm Therefore a grating bandwidth of 0 1 - 0 2nm FWHM is considered adequate With 1200 lines per mm at a wavelength of 1 3μm this implies a beam width perpendicular to the grating rulings of 0 5 - 1 0cm [1] In order to achieve this the diode should be mounted with its junction plane parallel to the grating rulings since,

i) the large beam divergence perpendicular to the junction plane will then illuminate the maximum number of lines

ii) tuning will be across the narrow face of the active region, thus decreasing the sensitivity to focus and grating misalignments

However in actual operation, it was confirmed that the diodes used emitted predominantly TE polarised light The highest first order grating reflectivity is obtained when the electric field vector is perpendicular to the grooves, which, for TE propagation in the diode, requires that the junction plane be oriented in this direction [2] Also, since the collimated beam profile was circular, with a diameter of 1cm, and, since the diode focus was under sensitive control using piezoelectric actuators, it was decided to use this configuration in order to minimise the cavity loss

Recalling Section 2 5, note that the coupling strength, C, into the cavity is given by

$$C = [1 - R^2]^{1/2} / R \qquad \textbf{Eqn: 4.1}$$

Therefore, in an external cavity, the laser diode facet facing the passive cavity must be antireflection, (AR), coated in order to maximise the intercavity coupling. The results presented here have been taken with a diode AR coated with a British Telecom Research Laboratory, (BTRL), proprietary AR coating. An important point to note at this stage regarding this coating is that at drive currents in excess of $1.5\,I_{th}$ the coating integrity can be lost and the coupling strength dramatically reduced [3]. Therefore all the results presented in this chapter were taken at drive currents of less than $1.5\,I^{m}_{th}$, where I^{m}_{th} is the threshold current associated with the m^{th} mode. This has serious consequences for the mode suppression ratio, (MSR), and is discussed later in this chapter. It is therefore important to monitor the output power during the alignment process.

The cavity is aligned by the use of an infra-red, (IR), viewer, to ensure that the beam coupled into the cavity is properly collimated. Then, with the grating in place, the returned diffracted beam is located and adjusted so that it falls on the collimating microscope objective. At this point it is critical that the output power be monitored since feedback can now occur. At the onset of feedback the drive current must be continuously adjusted during the fine alignment to ensure that it does not exceed the $1.5\,I_{th}$ limit.

4.2 Threshold current reduction in an external cavity.

In Section 2.5 it was demonstrated that the threshold current dependence of a laser diode on the facet loss is given by

$$\alpha_m = \frac{1}{2L} \ln\left[\frac{1}{R_1 R_{eff}}\right] \qquad \textbf{Eqn: 4.2}$$

where R_{eff} is the effective reflectivity brought about when the diode is operated in an external cavity. Assuming that the modal conditions are fulfilled, and therefore ignoring the effects on the output spectrum, R_{eff} can be thought of, to some degree, as restoring the original facet reflectivity. Therefore an AR coated laser diode in an external cavity would be expected to exhibit a lower threshold current and an increased efficiency than the same AR coated laser operated in isolation. It is worth noting that for the external cavity presented here it is unlikely that R_{eff} could ever be

greater than or even equal to the original, (uncoated), facet reflectivity (R_2) due to the low efficiency of the grating (≈30%), the losses due to collimation and the loss associated with the fact that only one mode (wavelength) is being selected for feedback Although operating in the cavity does decrease the power in these other modes, it does not eliminate them, thus they contribute to loss in the cavity Therefore a lowering of the threshold current, accompanied by an increase in the efficiency, is a useful indication of the presence of feedback The strength of this feedback is indicated by the magnitude of this reduction The threshold current was measured as follows For a given drive current, with the cavity aligned to a particular longitudinal mode, the output was focused onto a germanium detector It is important to ensure that the detector is operated over its linear region This is usually achieved by reducing the incident intensity through the use of neutral density filters At this position the light versus current (LI) curve was obtained Subsequently, with the external cavity blocked and therefore the diode operating in isolation, a second LI curve was obtained The results of this are presented in Figure 4 1 The results are as predicted, with a large increase in the observed efficiency of the diode on operation in the external cavity Note that in the absence of feedback there appears to be no

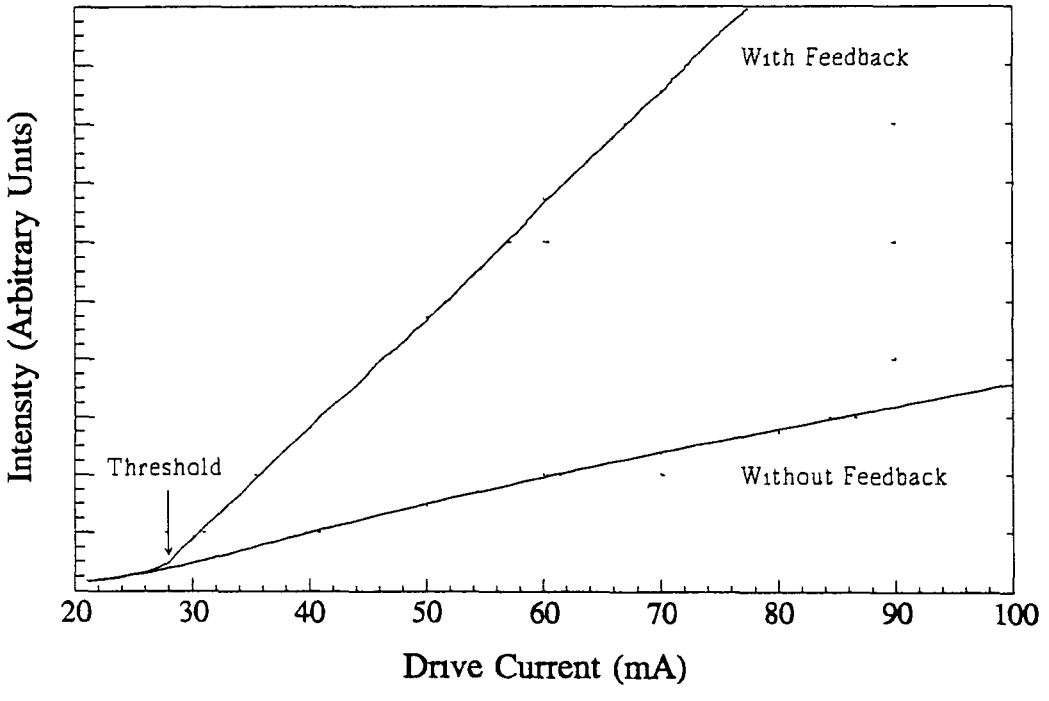

Figure 4.1· Light vs. current (LI) curves both with and without feedback.

sharply defined threshold current, indicating that the residual reflectivity of the laser facet is very low This tends to obscure the observable reduction in threshold current However this threshold reduction can be seen quiet clearly in Figure 4 4 later, where the threshold reduces as the efficiency of the feedback increases

4.3 Output spectra from the external cavity.

External cavity operation of a semiconductor laser diode offers single mode selectivity and wavelength tunability This longitudinal mode selectivity is due to the wavelength dependence of the effective reflectivity [4] The mode discrimination is brought about by the phase θ of the light coupling from the external cavity back into the lasing medium Side mode suppression is brought about by the fact that the active medium gain profile falls off as a function of wavelength and this interacts with the periodic loss profile However once a mode is selected, the higher photon population at this wavelength entering the active region increases the probability of a stimulated event at this wavelength This further reduces both the spontaneous output and also output into residual modes Additional mode selectivity can be brought about if the feedback is made wavelength dispersive This is the situation in the cavity presented here, where the reflector used in the cavity is a 1200 lines per mm diffraction grating The use of the grating has the further advantage that the output spectra can be tuned across the modes by rotating the grating In order to record the output spectra for various grating angles the grating spectrometer system shown in Figure 3 9 was used With the external cavity aligned initially to one mode the effect of grating rotation could be investigated The results of this investigation are shown in Figure 4 2

The top spectrum shows the output of the laser diode operated without feedback and at a drive current of 100mA As can be seen the laser exhibits the characteristic multimode operation The modal power distribution follows a Lorentzian distribution (shown in outline) as predicted in theory [4] The lower spectra were taken at 1 3 I^m_{th}, where I^m_{th} corresponds to the threshold current of the principle mode This principle mode is selected by the grating angle The mode suppression ratio, (MSR), averages to 10 3 for these tuned spectra The MSR could be improved were it not for the sensitivity of the AR coating to high optical powers, since, in the above threshold regime the power m the side modes saturates and only the principle mode increases with increasing current

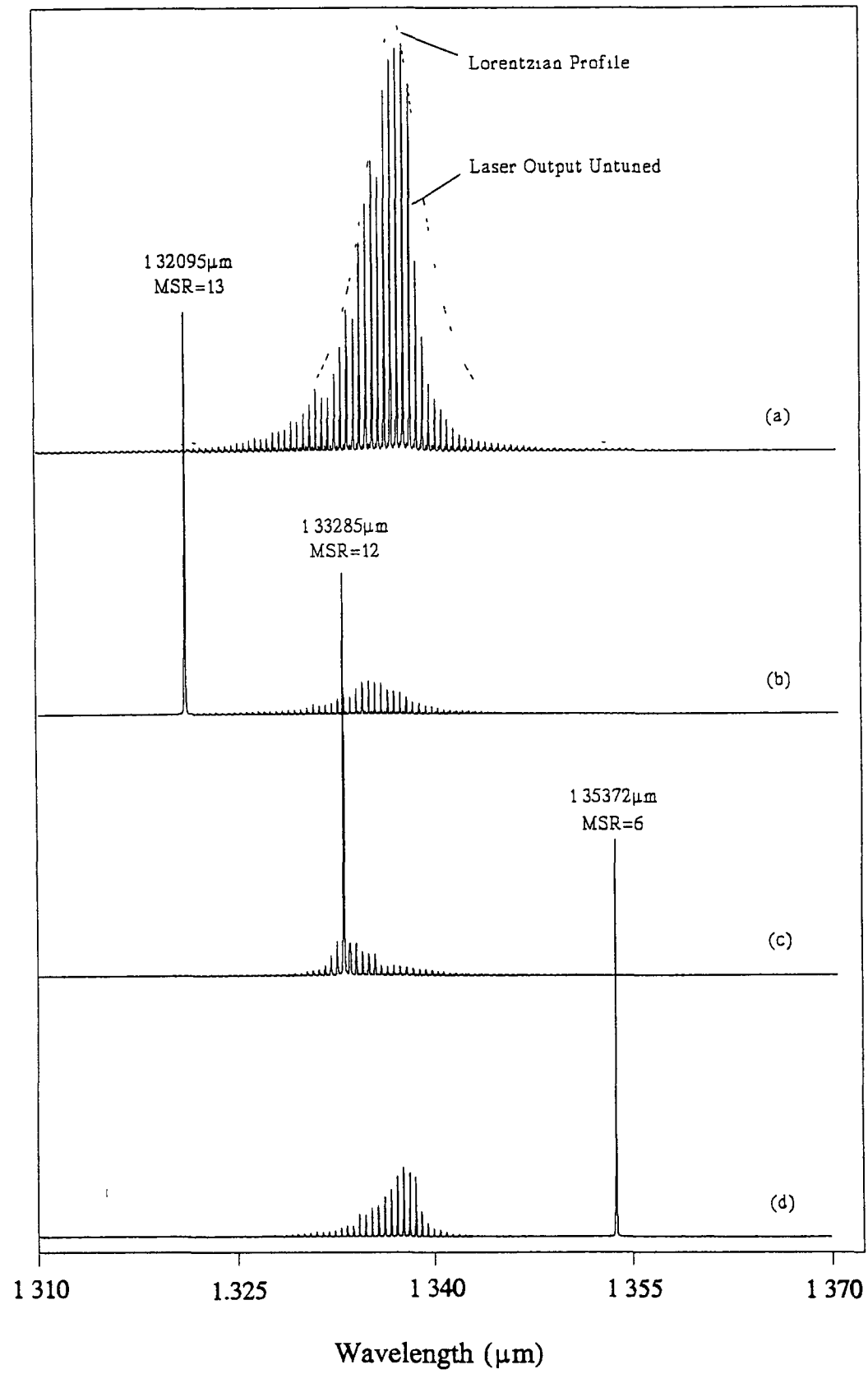

Figure 4.2: Output spectra from the external cavity· a) without feedback, b), c), d) with feedback from the grating at various angles.

4.4 Characterisation of the external cavity tuning range.

On operation in the external cavity the expected reduction in threshold current has been observed. The minimum threshold achieved was 27mA. This is in contrast with a threshold of approximately 18mA for similar laser diodes prior to AR coating, thus showing that the original threshold value is unlikely to be achieved in a cavity in this configuration. As was seen in Figure 4.1, the laser, when operated in isolation, exhibited no well defined threshold current due to the low residual facet reflectivity. Since the threshold current varies with the effective reflectivity (which is wavelength dependent) a plot of I_{th} versus wavelength is a very useful indication of the tuning range over which the external cavity operates. It is expected that mode selection at the extremes of this tuning range would be difficult due to lower gain and that therefore an increased threshold current would be observed.

In order to obtain this information a measure was first made of the total grating displacement over which feedback was achievable. LI curves were then taken as the cavity was tuned across this range. For each point, operating at $1.3\,I_{th}$ for that mode, a spectrum was recorded using the grating spectrometer system shown in Figure 3.9. This data was then imported into SPECTRA-CALC, a spectrum analysis package. The single mode wavelength for each case was noted and a plot of threshold current against wavelength was made. This is shown in Figure 4.3. For ease of reference, the differential micrometer reading, corresponding to the grating angle, is also presented on the same plot. As can be seen, feedback, and therefore single mode operation, is achievable over a 0.037μm (37nm) range from 1.317μm to 1.354μm for the diode used.

Recalling equation 2.26 it is seen that

$$I_{th} = q\,\gamma_e(N_{th})\,N_{th} \qquad \textbf{Eqn: 4.3}$$

where N_{th} corresponds to the threshold photon population at $G = \gamma$. Then

$$I_{th}(\lambda) \propto G(\lambda)^{-1} \qquad \textbf{Eqn: 4.4}$$

i.e. the threshold current is wavelength dependant due to the dependence of the gain on the effective reflectivity. Therefore the shape of the curve in Figure 4.3 reflects the shape of the gain spectrum associated with the external cavity. As can be seen the gain is reasonably flat over the central region of the tuning range. This should be

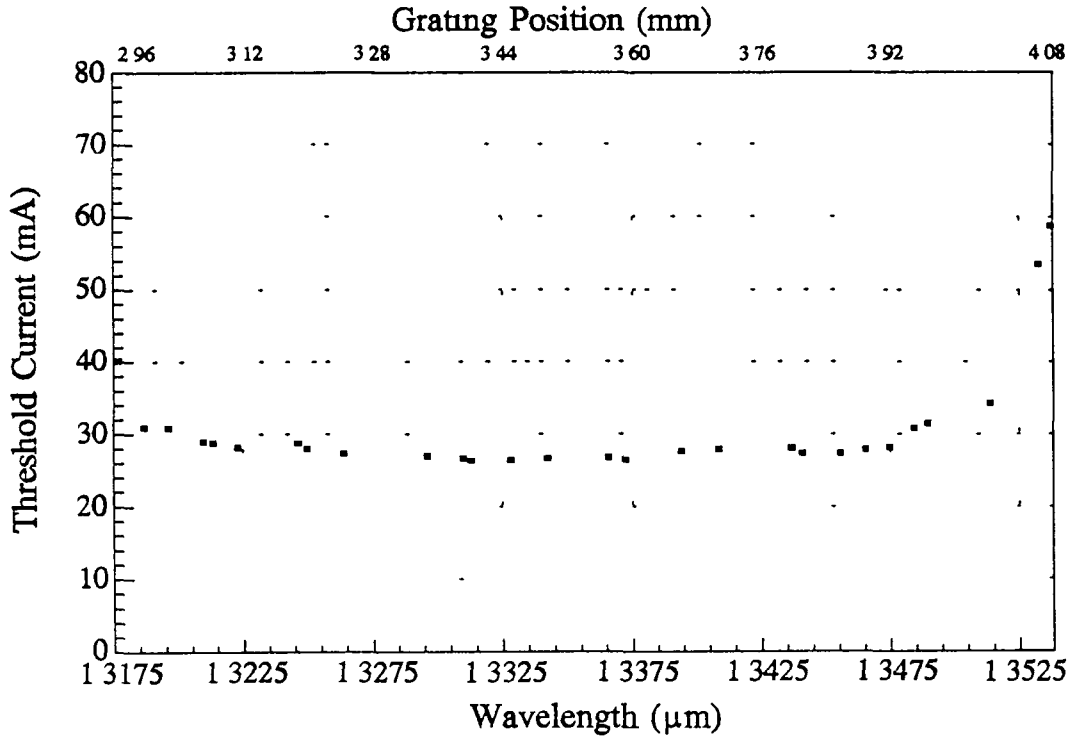

Figure 4.3: Grating tuning range of the external cavity laser diode.

reflected by the modes efficiencies The mode efficiency can be measured from the slope of the LI curve for that mode Several LI curves, taken over the tuning range, are shown in Figure 4 4 As is clear, the efficiencies at the tuning extremes are lower than those of the central region as expected Also the efficiencies over the central region are very similar to each other, reflecting the flatness of the gain spectrum

4.5 Effect of the injection current on the output spectrum.

Other methods, apart from rotation of the grating, by which the output wavelength of the laser can be tuned include device temperature and device current [5] Changing the device temperature changes the band-gap of the semiconductor material and also the optical path length due to thermal expansion It was initially hoped to investigate this temperature tuning, however it was found that the laser mount exhibited mechanical drift due to heater oscillations caused by the temperature controller This caused an oscillation of the focus position which was unacceptable for operation The cavity was therefore operated such that thermal equilibrium was achieved solely through the use of the Peltier heat pump. Also, temperature tuning is known to affect the life expectancy of laser diodes since a decrease of a factor of 5 is seen for a sustained

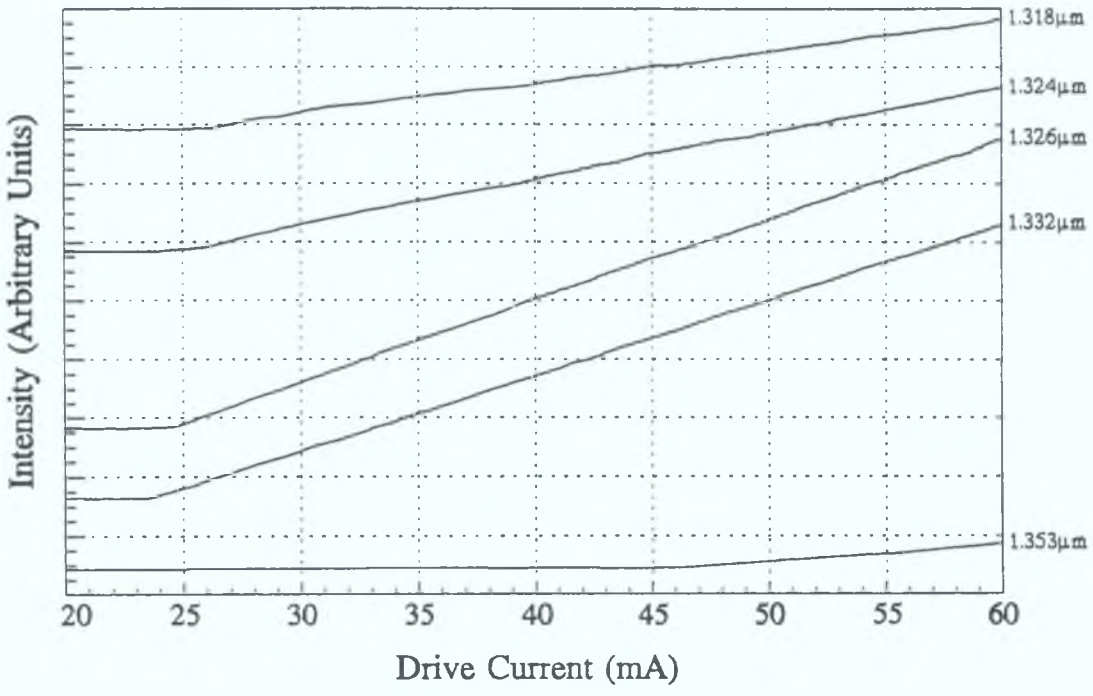

Figure 4.4: LI curves for various wavelengths over the tuning range.

temperature increase of 10°C [5]. In addition, since very little was known about the AR coating, the possibility of damage due to differences in the thermal expansion coefficients could not be ignored. Therefore large range temperature tuning was not attempted. However the effect on the output spectrum of the injection current was investigated.

Changes in the current affect both the diode temperature and the carrier density which in turn changes the refractive index, and these affect the lasing wavelength. For time scales longer than 1μs, however, this current tuning can be thought of as a method of changing the device temperature since the carrier density contribution to the refractive index is small [6]. With the laser tuned to a particular mode, the effect of the drive current was monitored using the grating spectrometer system. For each value of drive current the output spectrum was recorded. From these the single mode wavelength variation as a function of drive current could be seen. The resultant profile is shown in Figure 4.5. This form of tuning is a useful method of accessing wavelengths unavailable with the grating alone and is frequently used as such. The plot shows a tuning rate of 10GHz mA^{-1} (6.1×10^{-6}μm mA^{-1}). Figure 4.5 also demonstrates a feature common to temperature and current tuning, namely, mode hops. These unexpected

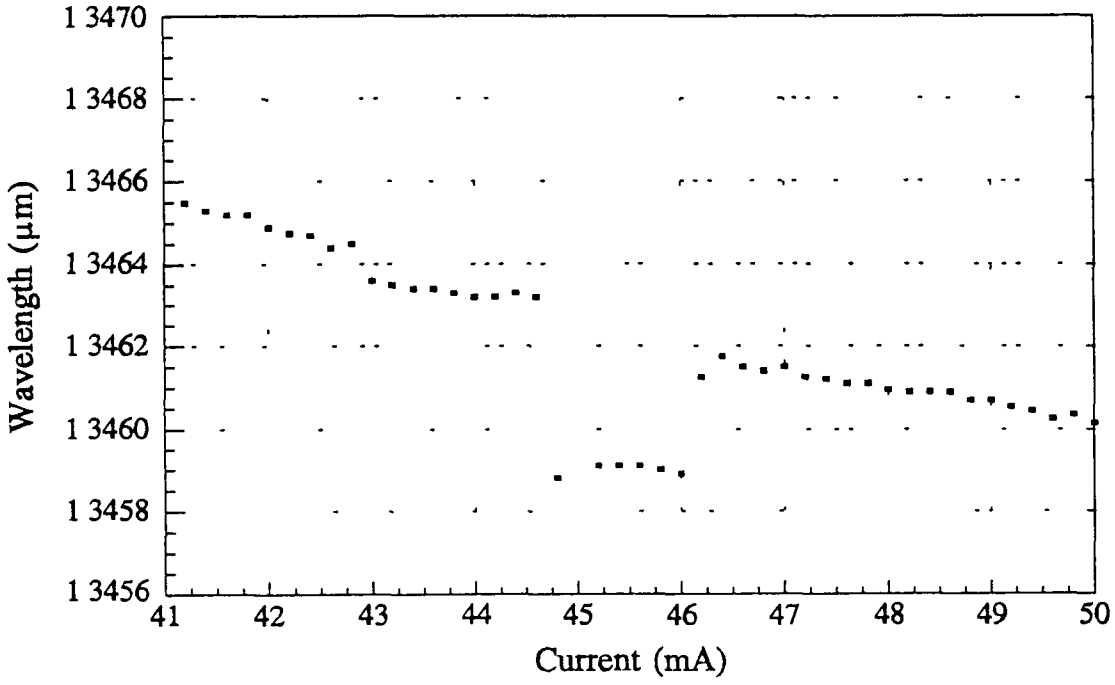

Figure 4.5. The effect of the injection current on the output spectrum.

wavelength jumps arise when the active medium refractive index is altered The losses for the lasing mode become greater than those associated with a nearby mode The laser output then jumps to this mode Typically the mode hop is of the order of 3×10^{-4}μm (0 35nm) as is found in Figure 4 5 [5] The presence of mode hops has been associated with the appearance of discontinuities, or kinks, in the LI curve Figure 4 6 shows such an LI curve This kink is caused by the change in efficiency, (which is proportional to cavity losses), which causes the mode hop Figure 4 7 shows the behaviour of the output spectrum of the laser under the same external cavity conditions as the LI curve was taken The spectral output demonstrated a repeatable jump of $8\ 5 \times 10^{-3}$μm (8 5nm) It should be noted, however, that mode hops of this magnitude are rare

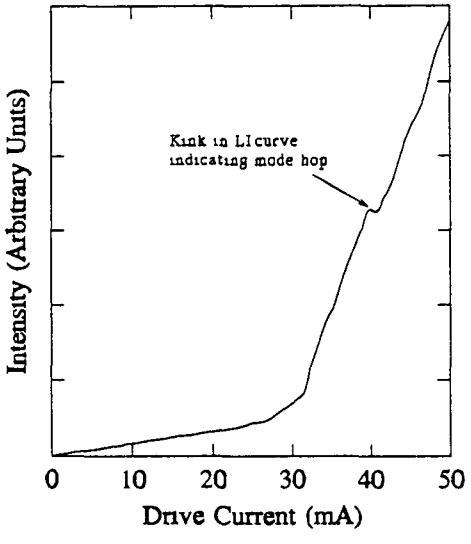

Figure 4.6: LI curve predicting mode hop.

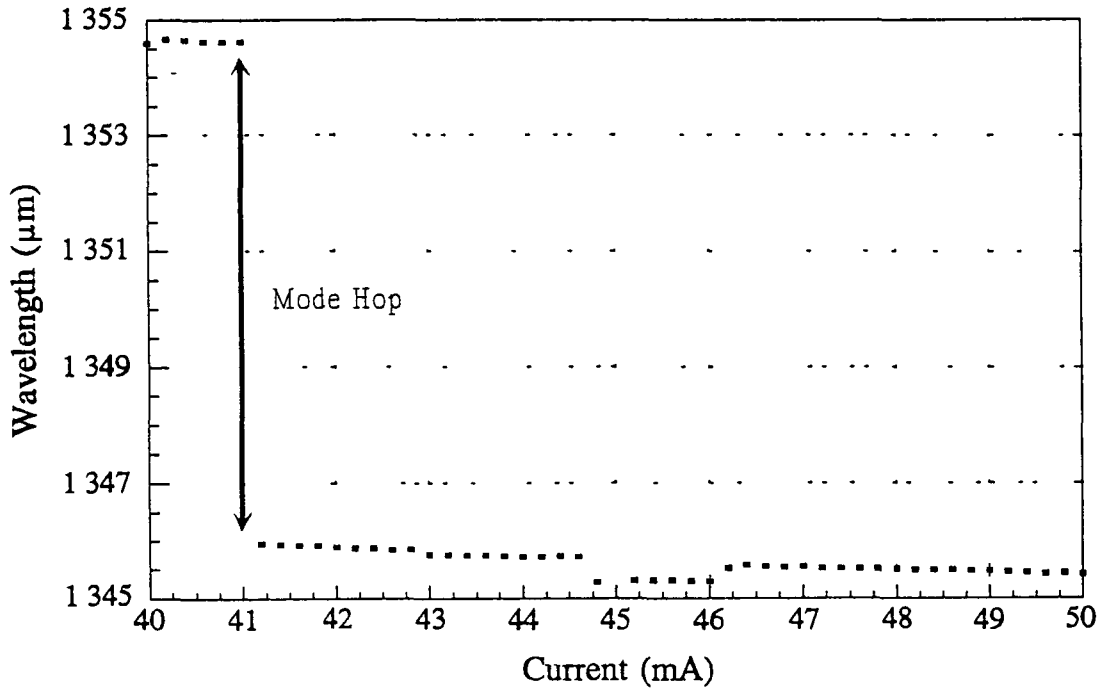

Figure 4.7: Tuning curve showing large mode hop over several longitudinal modes.

4.6 Linewidth.

Section 2 7 described the origin of the linewidth associated with laser diodes It also predicted the reduction of the linewidth by several orders of magnitude when such diodes are operated in external cavities Using the modified Schawlow-Townes formula the linewidth was shown to be

$$2\Gamma_m = \frac{\pi h \nu_m (\Delta \nu_c)^2}{P_m} n_{sp} \qquad \textbf{Eqn: 4.5}$$

At a cavity length, L, and a power of 0 1mW a linewidth of 3 3kHz is predicted for the external cavity presented in this work[1] In this calculation a measured grating efficiency of 30% was used T, the coupling efficiency, was estimated to be ≈2% when taking into account the transmission characteristics of the microscope objective used for collimation It is important to note that this represents strong feedback since the amount of feedback is larger than the coated facet reflectivity Obviously such narrow linewidths require special measurement techniques [7] However, since this

[1] See appendix A for additional laser parameters

system is designed for use as a source for spectroscopic applications, it is important to ensure that the laser linewidth is less than the instrument broadening of the spectrometer to be used Therefore an attempt was made to measure the linewidth using the BOMEM FTIR shown in Figure 3 11 With the external cavity tuned to a single mode the output was fibre coupled to the input of the FTIR Figure 4 7 shows the resultant spectra for cavity lengths of 55cm and 24cm The maximum resolution of the FTIR was 4 5GHz (corresponding to a wavelength resolution of the order of $2x10^{-5}\mu m$) It is clear therefore that the linewidth measurement is instrument limited

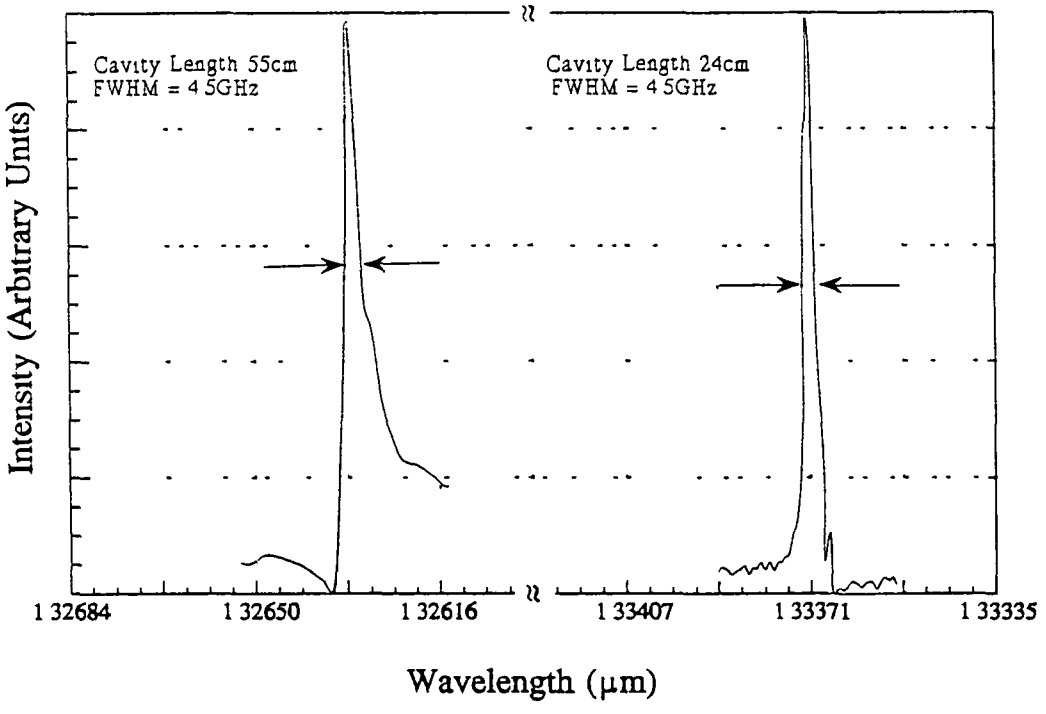

Figure 4.8: FTIR spectra for cavity lengths of 55cm and 24cm showing instrument limited linewidths of 4.5GHz.

to 4 5GHz Consequently it cannot be stated that the linewidth has been measured to any meaningful degree of accuracy Nevertheless the experimental results are presented in order to demonstrate that the external cavity is a useful narrow-linewidth source for use in a spectroscopic application based around the FTIR However the calculated linewidth for this work is in good agreement with both calculated and measured values of similar external cavity configurations [8]

4.7 Aging of laser diodes.

During the first 50 - 100 hours of operation in the life of a laser diode the tuning properties change dramatically [5] This is due to out-diffusion of the laser material from the active region, defect formation and defect migration Wavelengths, accessible at the beginning of a laser's life may become inaccessible as the device ages and vice versa This aging can be seen by comparing Figure 4 3 and 4 7 In Figure 4 7 the mode hop is from a wavelength of 1 3545μm As can be seen in Figure 4 3, this lies outside the initial tuning range of the device These two data sets were taken some time apart in the devices history Aging of the diode has pushed the output to longer wavelengths

4.8 Conclusion.

In this chapter the characterisation results obtained for the grating tunable external cavity have been presented Good agreement is found between the device behaviour and that both predicted theoretically and reported in literature The cavity was found to be tunable over a range of 0 037μm (37nm) by the use of the grating The effects of current tuning were investigated and a tuning rate of 10GHz mA^{-1} was established The problem of mode hops obscuring some of the tuning range was identified A device linewidth of 3 3kHz was calculated using the modified Schawlow-Townes formula Although this could not be verified experimentally it is in agreement with similar configurations previously published

References.

1 Zorabedian, P *Journal of Lightwave Technology*, **LT-10**, No 3, 330-335, March 1992

2 Fleming, M W and Mooradian, A, *IEEE J of Quantum Electron* **QE-17**, No 1, 1981

3 Sherlock, G In correspondence, BTRL, Ipswich, UK

4 Agrawal, G P and Dutta, N K , *Long wavelength semiconductor lasers* New York Press, 1986

5 Wittgrefe, F, Hoogerland, M D and Woerdman, J P *Meas Sci Technol* **2**, 1991

6 Weiman, C E and Hollburg, L *Rev Sci Instrum* **62**, 1 Jan 1991

7 Lin, T Y and Panais, J C *Conference record IMTC/84, IEEE Instrumentation and Measurement Technology* Conference, Boulder Co U S A March 1986

8 Wyatt, R and Devlin, W J *Electron Lett* **19**, No 3, 113, Feb 1983

Chapter 5: Conclusions

5.0 Summary of work.

The design and construction of a grating based tunable external cavity semiconductor laser has been presented in this work The current to the laser diode was supplied by a battery driven automatic current control circuit This ensured noise free continuous operation of the diode from 0 - 110 mA The temperature of the diode was initially controlled by the use of a PID controller at a set temperature of 21°C Heat evolved by the laser was drawn away using a Peltier-effect heat-pump This form of control was found to be inadequate since it introduced mechanical drift in the lasers position This was investigated and found to be due to the mount design rather than to any problems with the temperature controller itself Since the focused spot size of the lens used is of the order of the dimensions of the active region, a stabilised position is essential in order to avoid mode instabilities This form of control was therefore abandoned and the diode temperature allowed to reach an equilibrium position through the use of the Peltier alone

The external cavity was established between the antireflection coated (AR) laser facet and a diffraction grating, mounted in the Littrow geometry, used as the wavelength dispersive feedback reflector The laser output was coupled into this cavity through an antireflection coated achromatic microscope objective lens

The cavity was characterised using a 1 3μm laser diode provided by British Telecom Research Laboratories The influence of the AR coating on the coupling strength has been established It was shown that the device behaviour depended on the strength of this coupling The importance of optical feedback on the laser threshold current has been discussed through the concept of an effective reflectivity The expected reduction in threshold current due to optical feedback has been demonstrated experimentally

The tuning range available by rotation of the grating was measured using a grating based spectrometer system The external cavity demonstrated a tuning range of 37nm for the laser chip used The importance of the drive current on the output spectrum was also established A current tuning rate of 10 GHz mA^{-1} was found experimentally This was shown to be a useful method whereby gaps in the grating tuning range could be filled Discontinuities within the current tuning curve were shown to be due to the presence of mode hops These are caused by changes in the gain profile brought about

by a change in the optical path length due to thermal expansion The kinks on the light / current (LI) curve, indicative of the presence of mode hops, have also been demonstrated

Using the modified Schawlow-Townes formula, the linewidth of the single mode output of the external cavity was calculated to be 3 3 kHz This is in agreement with results presented for similar cavity configurations presented in the literature An instrument limited linewidth of 4 5 GHz (corresponding to $2 \times 10^{-5}\mu m$ @ $\lambda = 1\ 3\mu m$) was recorded when attempts were made to measure the linewidth using a Fourier Transform Infra-red Spectrometer

5.1 Suggestions for further work.

The problems of mechanical stability displayed by use of the temperature controller should be addressed To this end the laser mount should be redesigned One possible design would include fixing the diode stud to a material with a low coefficient of thermal expansion, e g INVAR which has $\alpha = 1\ 2 \times 10^{-6}\ K^{-1}$ compared to a value for copper of $\alpha = 1\ 7 \times 10^{-5}\ K^{1}$ Temperature control could then be achieved by a copper fin with an indium contact to the laser stud

The entire cavity should be temperature stabilised to reduce drift due to thermal expansion of the individual components or mounts This could be achieved by mounting the entire cavity on an INVAR rail and enclosing it in a temperature controlled case If this case were made gas tight the cavity could then be purged with dry nitrogen gas in order to remove water vapour The cavity could then be operated at lower temperatures without the problem of condensation on the facets

The tuning characteristics associated with a pulsed current configuration should be investigated The results presented here are for a device under continuous operation By using a pulsed current supply to drive the diode, the effects of refractive index changes, due to the change in carrier density caused by the current pulse, could be investigated It would also be possible to operate the laser at higher powers

The AR coating should be characterised, or on site AR coating of the facets with SiO should be undertaken This would enable a more extensive characterisation of the external cavity to be undertaken

An increase in the effective reflectivity is desirable in order to both extend the tuning range and increase the output power It is proposed that a gold coated grating, with

a high reflectivity and 1st order diffraction efficiency, would significantly increase the cavity reflectivity In addition, a high quality AR coated microscope objective should be used to collimate the beam into the cavity This would increase the coupling into the active region and further reduce the linewidth Further efforts should be made to determine the device linewidth experimentally This entails the design and construction of a heterodyne or homodyne beat frequency analysis system

Appendix A

Parameter	Symbol	Value
Cavity length	L	250μm
Active-region width	w	2μm
Active-layer thickness	d	0 2μm
Confinement factor	Γ	0 3
Effective mode index	$\bar{\mu}$	3 4
Group refractive index	μ_g	4
Linewidth enhancement factor	β_c	5
Facet loss	α_m	$45cm^{-1}$
Internal loss	α_{int}	$40cm^{-1}$
Gain constant	a	$2\ 5x10^{-16}cm^2$
Carrier density at transparency	n_0	$1x10^{18}cm^{-3}$
Non radiative recombination rate	A_{nr}	$1x10^{8}s^{1}$
Radiative recombination rate	B	$1x10^{-10}cm^3s^{-1}$
Auger recombination rate	C	$3x10^{-29}cm^3s^{-1}$
Threshold carrier population	N_{th}	$2\ 14x10^{8}$
Threshold current	I_{th}	15 8mA
Carrier lifetime at threshold	τ_e	2 2ns
Photon lifetime	τ_p	1 6ps

Table of typical InGaAsP laser diode parameter values

Appendix B

Quantity	Item	Supplier	Code
1	3'x1' Optical Breadboard	Photon Control	LCB-3-1
3	xyz Stage	Photon Control	TS-75-25Hxyz
2	Microscope Objective Adaptor Ring	Photon Control	AR50-RMS
1	Gimbal Mount	Newport Research Corp	605-2-OM
2	Fibre Launch Stage	Martok	/
20m	PCS Fibre	Tech Optic	C1-0125-80
1	Diffraction Grating	Optometrics	/
2	Differential Micrometer	Newport Research Corp	DM-13
2	Piezo Electric Actuator	LP Piezomechanik	/
1	Germanium Detector	Macam Photometrics	GD-101
2	Microscope Objective	Ealing Electro-Optics	25-0027

Required components for the external cavity laser diode

Parts List for Laser current source.

R_{set} x 10kΩ Pot
R_1 x 2kΩ
$R_{2,3,4,6}$ x 2 7kΩ
R_5 x 100Ω
R_{sense} x 2Ω
C_1 x 2 2μF
C_2 x 100μF
C_3 x 4 7μF
C_4 x 0 1μF
C_5 x 100nF
D_1 x IN4001
T_1 x BC108
$T_{2,3}$ x 2N3053
1 X 3140 Op-Amp
1 x 7805 Voltage Reg

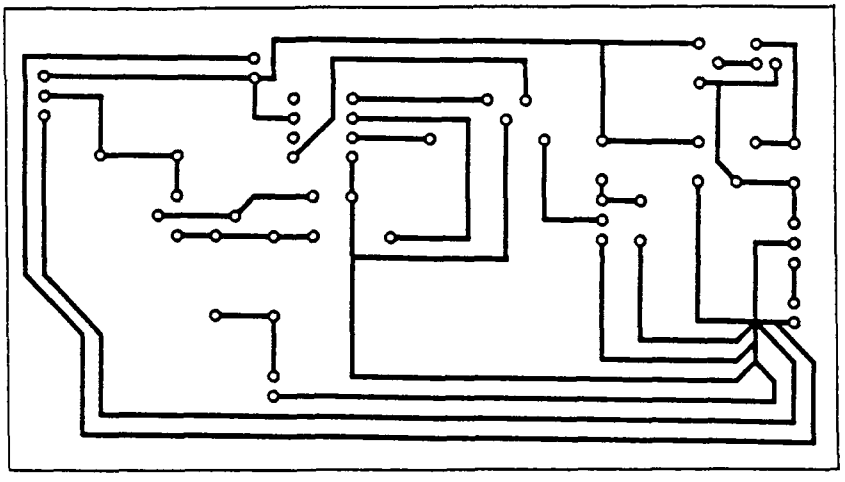

PCB foil for Laser Current Supply.

Parts List for Peltier current source.

1 x BC108
1 x TIP121
1 x Peltier Heat Pump
1 x 1 26Ω
1 x 240Ω
1 x ZN423 Voltage Reference Source
1 x 3140 Op-Amp

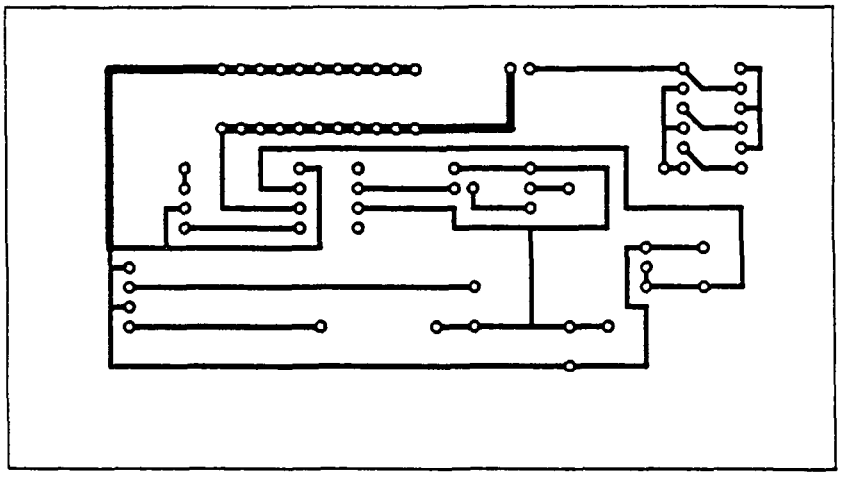

PCB foil for Peltier Current Supply.